Final Report

Simulation of Non-Point Source Pollution Processes in Song River

NATIONAL INSTITUTE OF HYDROLOGY
(An ISO 9001:2008 Institute under MoWR, RD and GR, Govt of India)
ROORKEE – 247 667 (UTTARAKHAND)

June 2025

Final Report

Simulation of Non-Point Source Pollution Processes in Song River

NATIONAL INSTITUTE OF HYDROLOGY
(An ISO 9001:2008 Institute under MoWR, RD and GR, Govt of India)
ROORKEE – 247 667 (UTTARAKHAND)

June 2025

CONTRIBUTIONS

Director	**Dr. M. K. Goel** **Director** **National Institute of Hydrology** **Roorkee – 247 667**
Head	**Dr. Y. R. S. Rao** **Scientist 'G' and Head** **Environmental Hydrology Division** **National Institute of Hydrology** **Roorkee – 247 667**
Principal Investigator	**Dr. Pradeep Kumar** **Scientist 'E'** **Environmental Hydrology Division** **National Institute of Hydrology** **Roorkee – 247 667**
Co-Investigators	**Dr. M. K. Sharma** **Scientist 'F'** **Environmental Hydrology Division** **National Institute of Hydrology** **Roorkee – 247 667**
	Dr. Rajesh Singh **Scientist 'E'** **Environmental Hydrology Division** **National Institute of Hydrology** **Roorkee – 247 667**
	Dr. Shakti Suryavanshi **Scientist 'C'** **Environmental Hydrology Division** **National Institute of Hydrology** **Roorkee – 247 667**
	Dr. S. K. Kumre **Scientist 'E'** **Environmental Hydrology Division** **National Institute of Hydrology** **Roorkee – 247 667**

CONTENTS

LIST OF TABLES

LIST OF FIGURES

ABSTRACT

The Himalayan rivers are particularly vulnerable to regional climate changes and anthropogenic influences, which can significantly alter both water quality and quantity, jeopardizing the fragile river ecosystems. This study investigates the hydrochemical characteristics of the Song River, a tributary of River Ganga focusing on non-point source (NPS) pollution, during the period June 2022 to November 2023. Monitoring of river discharge was carried out water samples were collected weekly during the monsoon (June to September), bi-weekly in the post-monsoon (October and November), and monthly during lean periods (December-May) from three monitoring stations. The study revealed that Biochemical Oxygen Demand (BOD) and Chemical Oxygen Demand (COD) eventually exceeded the criteria limits (3 mg/L for BOD and 10 mg/L for COD) prescribed by the Central Pollution Control Board (CPCB). The chemical composition of the river water at the monitoring stations revelated $Ca^{2+}$and Mg^{2+} as the dominant cations, while HCO_3^- and SO_4^{2-} were identified as the major anions. Gibbs plot suggesting the dominance of rock weathering as the major natural controlling mechanism of chemical composition in the basin. Carbonation and sulphide oxidation are two proton producing reactions controlling the chemical weathering processes. C-ratio plot suggested that dominance of carbonate dissolution in the tributary Suswa, while Song River showed dominance of sulphide oxidation, particularly in its upstream region. Spatial and temporal analysis identified nutrient pollution (NO_3^-, NH_4^+, PO_4^{3-}), organic loads (BOD, COD), and other parameters (TSS, Cl^-) as key contributors to water quality deterioration at the monitoring stations. A chemical mass balance (CMB) approach based on mass conservation has been applied for estimating the NPS pollution loads on the Song River. CMB calculations carried out for major cations such as (Na^+, K^+, Ca^{2+}, Mg^{2+} and NH_4^+) and major anions (Cl^-, SO_4^{2-}, HCO_3^-, NO_3^- and PO_4^{3-}) across a 21 km stretch of the river, encompassing approximately 305 sq. km. and observed that the contribution of uncharacterised load was maximum in dry season and minimum during monsoon season. Seasonal variations in ion concentration and flux were strongly correlated with hydrological processes, highlighting the need for comprehensive monitoring and management of NPS pollution in the Song River to safeguard its water quality and downstream impacts on the Ganga River system.

This study assesses the performance of the Soil and Water Assessment Tool (SWAT) in simulating streamflow and sediment for the Song River watershed, with a focus on calibration, validation, and sensitivity analysis. Thirteen parameters were selected for calibration, with

eight identified as highly sensitive, reflecting key hydrological processes of the area. The model was calibrated for the period 1974-1995 and validated from 1996-2004, with additional testing using field data collected in 2022-2023 through Acoustic Doppler Current Profiler (ADCP) measurements. Key model adjustments, such as the baseflow recession constant (ALPHA_BF) and channel roughness coefficient (CH_N2), were set to 0.05 and 0.04, respectively, to capture the area's groundwater dynamics and channel characteristics. The calibration results indicated a strong fit, with R^2 values of 0.77, NSE of 0.70, and PBIAS of 17.06, demonstrating good agreement between observed and simulated streamflow. Validation showed slightly lower but acceptable performance, with R^2 of 0.75 and NSE of 0.68. Further ADCP validation from field data showed R^2 values of 0.79 and 0.78 for two monitoring sites, confirming the model's reliability. Sediment yield simulations at site-2 yielded R^2 values of 0.70 and 0.59 for calibration and validation, with NSE values of 0.53 and 0.52, indicating the model's capability to simulate both streamflow and sediment accurately. These results demonstrate SWAT's practical utility for water resource management in similar data-limited regions.

CHAPTER - 1
INTRODUCTION

1.1 BACKGROUND

Rivers are the vital surface water resource, playing a crucial role in sustaining ecosystems, human settlements, and economic activities (Mishra and Saxena, 2024) around the world. They help to maintain ecological balance, provide water supply, host biodiversity, transport nutrients, replenish groundwater resources and soil fertility, regulate regional climate, hold cultural and spiritual significance, generate hydro-renewable energy, and enhance the natural beauty of the landscapes (Withers and Jarvie, 2008; Décamps, 2011; Pan et al., 2016; Parker and Oates, 2016; Tikuye et al., 2023; Usha and Singh, 2024). However, the escalating human population, developmental activities, substantial nutrient influx, point and non-point source pollution, changes in land use and land cover, and alterations in weather patterns, climate change have led to the degradation of river water quality (Khatri and Tyagi, 2015; Razali et al., 2018; Santy et al., 2020; Akhtar et al., 2021), consequently limiting its suitability for domestic, irrigation and industrial purposes (Singh et al., 2013; Matta et al., 2018; Mokarram et al., 2020). River pollution has significantly increased during the past few decades in many developing countries like India (Sharma et al., 2022) where modern agricultural and industrial practices have increased dramatically. The majority of the river pollution primarily attributed to anthropogenic activities, exacerbated by inadequate wastewater treatment facilities (Rakesh et al., 2022).

Water quality of riverine system has been deteriorated due to increment of pollutant inputs into the rivers. The nature of the pollutant acquits from point sources namely municipal sewage purification plants have a tendency to be unceasing, with inconsiderable changeability over time. The control of point sources can often be simple by treatment at the source and can be measured easily. Non point sources (NPS) pollutants are irregular, often sporadic and accompanied with unbalanced processes, such as intensive rainfall or major construction activities. Their contribution to the river system generally may be through by multiple factors including surface runoff, subsurface flow, or through the atmospheric deposition, that's why, NPS of pollution are difficult to measure and regulate. To address this issue, emphasis should be given on reducing pollutant

emissions into the environment, promoting sustainable land management practices, and modifying routine activities of large populations to minimize their impact on non-point pollution (Carpenter et al., 1998). In order to accomplish water quality goals, solely the control of point sources is not satisfactory and researchers have recognized that non-point sources of water pollution should be given similar attention. The efforts put on for the maximum probability of success for managing the pollution, it is necessary to acquire information about the spatio-temporal distribution of non-point loadings. However, this information is conceivably complex to obtain because of the resource constraints often placed on data pool and inconsistency of riverine loads (Reinelt and Grimvall, 1992). Currently, NPS are accountable for more than 50% of the problems relating to water quality issues (Jain et al., 2007). The implementation of systematic laws, standards and advanced engineering measures has significantly curtailed point source pollution.

A number of studies on the assessment of NPS pollution have been documented in the literature through variety types of NPS models (Leon et al., 2001; Kloiber, 2006; Shen et al., 2008; Lai et al., 2011; Wu and Chen, 2013; Chen et al., 2013; Zhai et al., 2014; Chen et al., 2015; Wang et al., 2019). The primary challenge facing researchers and decision makers is to estimate the point sources and non-point sources of pollution individually. Vast amount of data is required for NPS modelling to accurately assess their extent of contamination, in account of their dynamic nature influenced by hydrological processes and land use patterns. The agricultural farming methods and excessive irrigation aggravate the problem of NPS pollution across many river basins of the world (Srinivas et al., 2020).

To understand the aquatic sedimentary processes and the reactions involved thereof, a simple and effortless approach namely chemical mass balance (CMB) has been broadly used by different researchers during the previous years (Berndtsson, 1990; Jain, 1996; Jain et al., 1998; Kelley and Nater, 2000; Ismail and Ali, 2005; Jain et al., 2007; Mosley et al., 2012; Sharma et al., 2021).

Previous studies have investigated various aspects of the Song River and its tributaries, including Suswa and Sahastradhara. These research studies have focused on morphometric analysis (Pankaj and Kumar, 2009), biotic populations (Khanna et al., 2007), abiotic factors (Khanna et al., 2007; Bhutiani et al., 2014; Kaur and Naseer, 2023), heavy metal contamination (Bharti et al., 2014),

and plankton diversity (Chalotra and Rauthan, 2017). According to the Central Pollution Control Board (CPCB) report, the water quality of the Suswa River was documented as polluted (CPCB, 2019). Therefore, the sustainable management of these water resources relies heavily on its water quality and quantity, which fluctuates due to weather variations, geological factors and natural as well as anthropogenic activities (Akhtar et al., 2021). The Song River serves as a critical source of water for agricultural, domestic, and ecological purposes in the Doon Valley, but increasing human activities, such as urbanization and agriculture, pose challenges to its sustainability.

The present study aims to investigate the physicochemical parameters of Song River and its major tributary Suswa across three monitoring stations i.e. two stations along the Song River one each before and after the confluence of Suswa and Song Rivers and one station on Suswa River. To investigate potential sources of non-point source pollution, chemical mass balance application based on law of conservation of mass applied on river Song, a tributary of the Ganga. This approach not only provides a detailed characterization of the chemical composition of river water but also facilitates to investigate the temporal variations in water quality and further estimate the contribution of NPS loads. Additionally, the study highlights the hydrochemical characteristics of the Song River and its tributary, the Suswa River, thereby establishing baseline data on its current status.

Accurate estimation of streamflow and sediment generation is crucial for effective water resources management. Hydrological models serve as fundamental tools for simulating these processes and have been extensively utilized for both change detection and attribution in catchment systems (Folton et al., 2015; Hassan et al., 2010; Vandenberghe et al., 2006). Inappropriate application of these models may result in erroneous understanding and suboptimal policy recommendations. Daggupati et al. (2015) assert that the requisite modeling accuracy may vary for different applications, contingent upon the risk associated with actions that follow model implementation (e.g., explanatory, planning and/or regulatory).

Surface water resources, particularly rivers, are essential for sustaining ecosystems, human settlements, and economic activities worldwide (Mishra and Saxena 2024; Kumar and Sen 2023). Global warming-induced changes in weather patterns, urban expansion, industrial growth, and

agricultural chemical use are transforming water resources (Joseph et al., 2018; Kaur and Sinha, 2019). Numerous areas face freshwater shortages or contamination issues. Hydrological elements such as evaporation, transpiration, soil moisture, and runoff are highly responsive to slight changes in temperature and precipitation (Brutsaert, W, and Parlange, 1998; Seneviratne et al., 2010). Consequently, addressing water resource challenges, including the effects of urban development, alternative management approaches, and future climate variations on streamflow and water quality, necessitates a comprehensive understanding and accurate modeling of Earth surface processes at the catchment level (Kumar and Paramanik, 2020; Iwanaga et al., 2020; Gassman et al., 2014; Koltsida et al., 2023). Examining various components of the hydrological process is necessary to evaluate and quantify sediment and auricular chemical yields (Ghoraba S.M., 2015).

Due to the complexity of hydrological processes, various models have been developed over time to facilitate the comprehension of the hydrological system (Arnold and Allen, 1996; Sahu et al., 2016). These hydrological models are essential tools for evaluating catchment behaviour, informing decisions on water resource projects, flood control, pollution management, and numerous other applications (Gupta et al., 2024; Pérez-Sánchez et al., 2019; Kumar and Sen., 2024). Among these, semi-distributed hydrological models can simulate water balance spatially by accounting for various soils, land uses, topographical features, and climate conditions (Rafiei et al., 2017). The semi-distributed hydrologic model SWAT is renowned for providing detailed information on water resources in a river basin and projecting the impact of land use changes and management practices on water quantity and quality (Janjić, and Tadić 2023; Gelete et al., 2023; Narsimlu et al., 2015). Researchers have applied the SWAT model across various regions, from arid and semi-arid to humid and tropical (Nguyen and Kappas, 2015; Samimi, 2020). Schuol et al. (2008) assessed the distribution of blue and green water in Africa; Phuong et al. (2014) utilized SWAT to estimate surface runoff and soil erosion in a small part of Vietnam. Understanding runoff and sediment yield dynamics in watersheds is crucial for effective management, especially in data-scarce regions such as the Western Himalayan area. Jain et al. (2010) employed SWAT to estimate runoff and sediment yield in the Suni to Kasol watershed, achieving satisfactory R2 coefficients for both daily and monthly values. Similarly, Agrawal et al. (2011) simulated surface runoff and sediment yield in the Chhokranala watershed, emphasizing the impact of calibrated Manning's 'n' values on sediment yield. Aawar and Khare (2020) utilized the SWAT model to analyze the climate

change impact on the streamflow of the Kabul River; Bouslihim et al. (2016) opted for the SWAT model to access the hydrological components of the Sebou watershed (Morocco). The SWAT model can also simulate basin hydrology in terms of both quantity and quality by incorporating agricultural practices, point sources, and non-point sources.

1.2 PROBLEM DEFINITION

Increasing population and subsequently increasing water, food and energy demands have put tremendous pressure on the water resources. The problem is more substantiated by the increasing consumption of the products with high water footprints. The food and energy demands of rapidly increasing population have caused intense agriculture, industrialization and urbanization. This has resulted in indiscriminate discharge of municipal and industrial wastes. Municipal wastes being biodegradable produce a series of directional but predictable changes in water bodies. Industrial effluents are responsible for pollution to a lesser extent but the effects produced by them may be more serious as nature is often unable to assimilate them. Agriculture is also responsible for degrading the water quality through leaching and runoff from agricultural fields and animal husbandry units, which contain predominantly organic compounds from the use of mineral fertilizers and chemical pesticides. These pollutants ultimately contaminate aquifer system due to surface and groundwater interactions.

The planning of water as a national resource is not merely a question of ensuring the availability of water in the right quantity at the right time for diverse purposes, but also ensuring the right quality for the intended use. Further, for any proper water resources planning, whether long or short term, before going into alternative plans for development, it is very essential to assess water quality problems together with hydrological analysis.

Since, point source pollution meets the river at known locations, it may be addressed by STPs or ETPs. Non-point source pollution reaches the river through the landscape after following a number of hydrologic, physical, chemical and biological processes. Hence, it is very complex to assess the causes and plan for its remediation. Very few assessments of non-point source pollution have been made in Indian rivers and they are mostly limited upto quantification of pollutant loads through

the flux balance approach. Therefore, this study is being envisaged to simulate the non-point pollution process in a lower Himalayan catchment to identify the sources and causes of non-point source pollution.

1.3 OBJECTIVES

The primary objective of this study is to apply the SWAT model to simulate the hydrological processes and to simulate the non-point source pollution processes in the Song River catchment. The specific objectives for this study are as follows:

a. Assessment of the point and non-point pollutant loads in the Song river catchment
b. Simulation of various hydrological processes in the Song river catchment
c. Simulation of non-point source pollution process for sediment and nutrients in the Song river catchment

CHAPTER – 2
STUDY AREA

2.1 THE SONG RIVER CATCHMENT

The Song River, originating from various small streams in the Dhanolti mountain range and merging with Sahastradhara streams, flows down to the Doon valley basins before eventually joining the Ganga River. Known for its picturesque surroundings, the Song River in Dehradun is particularly renowned for its plentiful natural sulphur springs. These springs emerge from mountain fissures and feed into the main watercourse, enriching the river with sulphur. Visitors flock to immerse themselves in the mineral-rich waters, as sulphur baths are thought to alleviate various health issues, particularly skin conditions. Situated at 30º28' latitude and 78º8' longitude, the Song River is vital to the communities of Raiwala, Doiwala, Chiddarwala, and Lacchiwala, serving as their primary water source along its 107 km journey. It converges with the Ganga River at 78° 14' 54" longitude and 30° 02' 02" latitude, just upstream of Haridwar near the Satyanarayan GandD station maintained by CWC, after passing through the Satyanarayana area (Figure 1).

A significant tributary of the Song River is the Suswa River, which originates in the clayey depression of the Mussoorie range. It drains the eastern part of Dehradun city and joins the Song River southeast of Doiwala. The catchment area includes two major urban settlements: Dehradun and Doiwala. The Rispana and Bindal, two primary drainage networks, carry municipal sewage from these urban areas and discharge into the Song River via the Suswa River. The region experiences an average annual rainfall of approximately 1451 mm, with about 1181 mm (81%) occurring during the monsoon season. Consequently, July and August are the wettest months of the year.

The Song River is a prominent perennial tributary of the River Ganga, located in the Dehradun district of Uttarakhand, India stands as the largest river in the Doon Valley (Sharma et al., 2022). The Song River basin (Figure 1) covering approximately 970 sq. km, is characterised by diverse landscape of steep slope in the upper course and relatively flat terrain downstream. The Song River originates through various small rivulets from mountainous range of Dhanolti near Surkanda peak

(at an elevation of about 2700 m above m.s.l.) in Tehri Garwal district, Uttarakhand. After traversing the steep terrain of its upper course, the Song River enters the plains, flowing in a north-south direction through a wide-open valley (Khanna et al., 2007). River Suswa is the right bank tributary and the Jakhan Nadi is the left bank tributary. Jakhan Nadi remains dry throughout the most of year except a few days during high intensity rainfall in monsoon season. Suswa River, a major tributary of Song originating from a clayey depression near the Asan River, drains the eastern part of Dehradun city receiving municipal sewage from the Rispana and Bindal streams. It forms a deferred junction with the Song River in Kans Rao forest near Doiwala (CPCB, 2019). Thereafter, travelling a distance of about 19 km, Song River finally assimilates with river Ganga just upstream of Haridwar near Raiwala (Khanna et al., 2007; Sharma et al., 2022).

The Song Rivers provides essential freshwater for domestic use, irrigation, and fisheries across the Doon valley. The catchment area is home to significant urban settlements, including Dehradun and Doiwala, and is impacted by industrial activities, such as a distillery and a sugar unit. The river basin's geology, comprising various alluvial formations, reflects complex geological processes. The spring-fed Song River, known for its natural sulphur springs, attracts visitors seeking therapeutic baths believed to alleviate skin ailments. This river is crucial for the communities of Raiwala, Doiwala, Chiddarwala, and Lachchhiwala, serving as their primary water source along its 79 km downstream journey to the Ganges, merging just upstream of Haridwar.

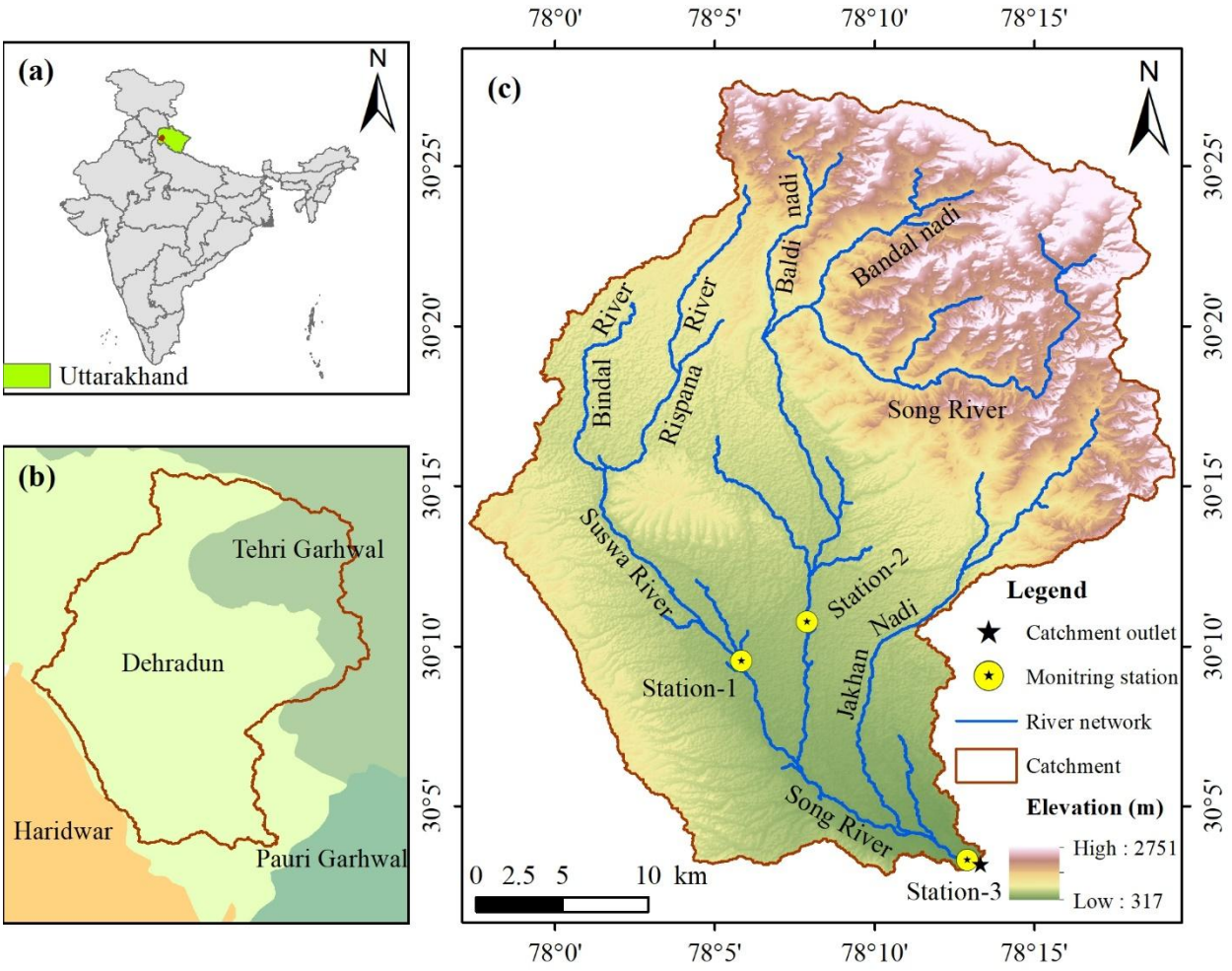

Figure 2: Study area map of Song River catchment showing the monitored stations along the Song River and tributary Suswa

The region experiences a subtropical monsoon zone, receives an average annual rainfall of approximately 1451 mm, with more than 81% of the of precipitation occurred during July and August. The climate within the catchment ranges humid continental to tropical depending upon the altitude and season. The average seasonal temperature ranges between 18.6°C – 34.3°C in summer season while winter fluctuates between 4°C to 19°C, influenced by the altitude and proximity to the Himalayas. The hydrological regime of the Song River, with peak discharge

occurring during monsoonal rainfall while the significantly reduced flow during lean periods (December to May), primarily sustained by baseflow contribution and groundwater inputs.

2.2 DESIGN OF MONITORING STRATEGY AND STATION DESCRIPTION

The River Song and its tributary, the Suswa River, were regularly monitored over two monsoon years (June 2022 to November 2023). To capture the pollutant loads through sewage from Dehradun and Doiwala cities, the industrial units (one distillery and one sugar processing unit) and the agricultural field, three strategic monitoring stations were selected: one on the Suswa River and two on the Song River (one each before and after the confluence of Suswa and Song Rivers) as shown in Fig. 1. The purpose of selecting these three stations to assess the non-point source (NPS) pollution loads across a 21 km stretch of the river, encompassing approximately 305 sq. km. These stations were selected for their accessibility near road bridges, facilitating regular monitoring during the monsoon season. Discharge measurements and grab water sampling were conducted weekly during the monsoon periods (June-2022 to September-2022 and June-2023 to September-2023), bi-weekly in the post-monsoon periods (October-2022 to November-2022 and October-2023 to November-2023), and monthly during lean periods (December-2022 to May-2023) to evaluate the variations in point and non-point source pollution loads. The details of selected monitoring stations are provided in Table 1 and illustrated in Figure 1.

Table 2: Descriptive characteristics of the selected monitoring stations

Station Code	Sampling Station Name	Stream	Latitude (Decimal Degrees)	Longitude (Decimal Degrees)	Elevation (m above m.s.l.))	Distance from Confluence of Suswa and Song Rivers
Station 1	Suswa Bridge, Doiwala	Suswa	30.15864	78.09739	452.04	7 km U/S
Station 2	Song Bridge, Doiwala	Song Upstream	30.17915	78.13162	486.32	8.6 km U/S
Station 3	Song Bridge, Nepali Farm, Raiwala	Song Downstream	30.05506	78.21517	346.35	12 km D/S

- ***Suswa Bridge near Markham grant, Doiwala (Station 1)***: Dehradun and Doiwala are the two major developed emerging urban settlements located in Suswa River catchment. Bindal and Rispana Rivers are two main tributaries of Suswa River which carry all the municipal sewage of Dehradun city and drain it into Suswa River at Mothrawala. Suswa bridge is located at (30.15864° N, 78.09739° E) at an elevation 452.04 m on Suswa River (near Sashastra Seema Bal campus, between Doiwala and Bullawala). The catchment area of Suswa River at this sampling station is about 240 sq. km. Sampling at this location also helped for calculating the pollutant load in Suswa River before its confluence with Song River. The water quality at this location reflects the impact of treated and untreated sewage of Dehradun city after the Mothrawala Sewage Treatment Plant.
- ***Song upstream near Doiwala (Station 2)***: The upstream area of the Song River covers approximately 430 sq. km, with a key location near the geographical coordinates 30.17915° N, 78.13162° E just upstream of the Doiwala Bridge on Song River. One of its tributary, the Baldi River, also known as Sahastradhara, originates from the Sahastradhara region is particularly notable for its abundant natural sulfur springs enhancing its mineral content and contributing a substantial portion of water to the hydrological complexity of the Song River system. Sampling at this location also helped for calculating the pollutant load in Song River before the confluence of Suswa River.

- ***Song downstream near Nepali Farm, Raiwala (Station 3)***: The last sampling point was chosen at the geographical coordinates 30.05506°N, 78.21517°E, which is located approximately 4.5 km upstream from the confluence with the Ganga River. This station is situated near Nepali Farm, Raiwala, at the Satyanarayan temple, covering a catchment area of 970 sq. km.

CHAPTER – 3
METHODOLOGY

3.1 MONITORING OF DISCHARGE AND WATER QUALITY PARAMETERS OF THE RIVER

Monitoring discharge is crucial for calculating pollutant loads. We utilized the SonTek FlowTracker2 ADV (Acoustic Doppler Velocimeter) and SonTek River Surveyor-M9 Acoustic Doppler Current Profiler (ADCP) to measure real time velocity and discharge. The SonTek FlowTracker2 ADV measures velocities ranging from 0.001 to 4 m/s and is used during low-flow conditions, applies the mid-section method for discharge calculations. However, during the monsoon season, when river velocities increase significantly, the FlowTracker2 ADV wading rod could not withstand the high flow rates. Under these high-flow conditions, we deployed a boat-mounted RiverSurveyor-M9 ADCP. This ADCP allowed us to measure both velocity and discharge up to 80 m depth effectively, adapting to the dynamic flow conditions typical of the monsoon period.

The grab water samples were collected in high-density polyethylene (HDPE) bottles, pre-cleaned with distilled water, and rinsed with the sampled water (APHA, 2023). Water samples were taken from a depth of 10-15 cm to minimize interference from surface debris (Sharma et al., 2021). River water quality parameters monitored included pH, electrical conductivity (EC), total suspended solids (TSS), Alkalinity, Hardness, cations like sodium (Na^+), potassium (K^+), calcium (Ca^{2+}), magnesium (Mg^{2+}), ammonium (NH_4^+), and phosphate (PO_4^{3-}), anions like bicarbonate (HCO_3^-), chloride (Cl^-), fluoride (F^-), sulphate (SO_4^{2-}), nitrate (NO_3^-) and nitrite (NO_2^-), dissolved oxygen (DO), biochemical oxygen demand (BOD) and chemical oxygen demand (COD). On-site measurements of pH and electrical conductivity (EC) were conducted using a portable water analysis kit (make: Hach, model: HQ30d Portable Multi-Parameter Meter). Samples were preserved with appropriate reagents (conc. H_2SO_4 for COD analysis; alkaline $MnSO_4$ and alkali azide (KI) for determination of DO) and transported in an insulated icebox, refrigerated at 4°C until laboratory analysis.

In the lab, water samples were filtered through 0.45-micron filter paper using electric vacuum pump to remove suspended sediments. The filtered water samples were analyzed for ions and alkalinity using an Ion Chromatograph (make: Metrohm; model: 930 Compact IC Flex, Switzerland) with Auto Titrator. DO was analyzed through the Winkler's titration method, while BOD was estimated using the 5-day incubation method followed by Winkler titration using digital titrator to enhance accuracy and precision. COD was estimated using UV spectrophotometer (make: HACH; model: DR6000) at 600 nm wavelength followed by closed reflux colorimetric method. The concentration of TSS in water samples was estimated by drying the suspended particles retained on pre-weighted filter paper dried at 104°C to a constant weight. All procedures adhered to APHA guidelines for evaluating physicochemical parameters. The ionic balance error of each analysis was calculated < ±10% using the Normalized Inorganic Charge Balance (NICB) equation 1 confirming consistency and quality of analytical results.

$$NICB = [(\mathrm{TZ}^{+} - \mathrm{TZ}^{-})/(\mathrm{TZ}^{+} + \mathrm{TZ}^{-})] * 100$$

Where TZ^{+} and TZ^{-} are sum of all cations and anions expressed in $mEq.L^{-1}$, respectively. The details of preservatives and instruments used to evaluate physio-chemical parameters are in accordance with APHA (2023).

3.2 STATISTICAL ANALYSIS

The statistical analysis of various water quality parameters collected during the monsoon season across three stations (Sta-1, Sta-2, Sta-3) were conducted using a one-way ANOVA to access the significant difference from their means. P value less than α value of 0.05, where α indicates a five percent deviation of the mean value are considered as significant in the statical analysis were depicted in Table 2.

The parameters such as Alkalinity, Hardness, Na^{+}, K^{+}, Ca^{2+} and Mg^{2+} shows the p-value smaller than α, indicating that there is a significant difference between the three stations. The F-value is much larger than the F-critical (3.094), providing strong evidence that the group means are significantly different from one another. Similarly, HCO_3^{-}, Cl^{-}, SO_4^{2-}, NO_3^{-}, NO_2^{-}, NH_4^{+}

concentrations displayed significant variations, with F-values, further indicating that anthropogenic activities or natural factors might be influencing the water chemistry differently at each station. Additionally, parameters like DO, BOD, and COD revealed significant spatial differences, indicating varying levels of organic pollution across stations.

The parameters like pH, TSS, F^- and PO_4^{3-}, the p-value higher than the significance level (0.05) indicating there is no statistically difference in the values across the three sampling points. The F-value lower than the F-critical, reinforcing that there is not enough evidence to conclude that the mean values differ significantly between the three stations. The variation in TSS is likely due to random fluctuations rather than real differences between the stations.

Table 3: One-way ANOVA test

Parameter	**P-value**	**F-value**	**Std. Dev**	**Mean**	**C.V. %**
pH	0.6894	0.373	0.451	6.93	6.50
EC	0.0000	14.11	161.32	618.9	26.05
TSS	0.2924	1.25	790.91	386.9	204.35
TDS	0.0000	13.94	119.45	492.9	24.2
Alkalinity	0.0000	61.16	53.93	180.3	29.92
Hardness	0.0006	8.03	70.83	282.9	25.06
Na^+	0.0000	121.48	5.13	15.4	33.33
K^+	0.0000	90.03	2.14	6.27	34.18
Ca^{2+}	0.00029	8.89	16.76	69.91	24.00
Mg^{2+}	0.00405	5.85	7.53	26.93	27.98
HCO_3^-	0.0000	61.16	65.77	196.5	33.47
Cl^-	0.0000	110.84	7.79	3.75	44.87
SO_4^{2-}	0.0000	35.48	18.06	75.74	23.87
NO_3^-	0.0000	19.16	4.85	6.17	78.75
F^-	0.779	0.25	0.52	0.16	3.13
NO_2^-	0.00028	9.29	1.82	0.21	19.53
NH_4^+	0.0000	18.06	1.13	0.55	51.60
PO_4^{3-}	0.3645	1.03	0.63	0.49	47.20
DO	0.0034	6.06	1.10	7.43	19.88
BOD	0.0000	11.45	3.11	4.52	68.80
COD	0.0018	7.30	11.37	19.15	59.33

3.3 CHEMICAL MASS BALANCE APPROACH FOR ASSESSING THE NON-POINT POLLUTION LOADS

Small catchment hydrology research often utilizes a basic mixing model technique known as the input-output water and solute mass balance (Hooper et al., 1990; Christophersen and Hooper, 1992). This simple mass balance approach can effectively model in-stream dynamics and predict nutrient flow in rivers (Berndtsson, 1990; Jain, 1996; Jain et al., 1998; Kelley and Nater, 2000; Jain et al., 2000; Ismail and Ali, 2005; Jain et al., 2007; Alam and Dutta, 2012; Mosley et al., 2012; Angello et al., 2020; Sharma et al., 2021). A key aspect of water quality engineering is the estimation of input mass loading, or the total mass of a substance discharged per unit time into a water body (Jain et al., 2000; Jain et al., 2007). The input load for specified sources with continuous flow is determined using the following equation:

$$L(t) = Q(t) * C(t)$$

Where, L(t) is the mass rate (load) being transported of the input (MT^{-1}), while Q(t) and C(t) represents the input flow rate (L^3T^{-1}) and the input concentration of substance (ML^{-3}) respectively at a specific time t. The fundamental idea in describing the input discharge of material into a river is to apply a mass balance equation across various reaches of the river.

To estimate the contribution from both point sources and non-point sources in a river system, the indirect measurement, chemical mass balance (CMB) approach is a widely used for quantifying the pollutant loads in a river reach between two monitoring stations using the following equation:

$$Q_D C_D - Q_U C_U = \sum_{i=1}^{n} Li - \sum Consumption + \sum In\ situ\ generation$$

Where, Q_D and Q_U depicts the flows at downstream and upstream stations, C_D and C_U are the concentration of selected parameter in the river water at downstream and upstream stations, and $\sum_{i=1}^{n} Li$ can be considered as contribution from both point sources and non-point sources into the river, neglecting consumption and/or generation between two monitoring stations (Makanda et

al., 2023). This approach may not estimate an accurate estimation of loading for any contaminant that undergoes significant volatilization or degradation unless the travel time between upstream and downstream locations is minimal compared to the rate constant for loss/gain. This also applies for substances that undergo sedimentation from the water column (Jain, 1996; Angello et al., 2020).

The above CMB equation (2) provides a robust framework for designing studies that enhance pollutant source apportionment accuracy, especially in large-scale assessments. The likelihood of inaccuracies increases when calculating the total contributions from both point and non-point pollution sources through the aggregation of individual load data from multiple sources. Such calculations typically involve large datasets, which are prone to errors arising from analytical limitations and systematic uncertainties. The inherent advantage of this equation lies in its ability to minimize errors introduced during the analytical processing of numerous individual samples, which can lead to significant inaccuracies in cumulative load calculations.

The efficiency of chemical mass balance modelling to assess the contribution of non-point sources of pollution is influenced by the following factors: (i) selection of river stretch and identification of input point sources of pollution, (ii) selection of sampling stations and monitoring frequency of discharge and water quality parameters, (iii) estimation of water quality data (of chemical species) analyzed in the laboratory (Angello et al., 2020; Sharma et al., 2021).

3.4 SWAT MODEL SET UP

3.4.1 Spatial database

Digital Elevation Model (DEM) are critical tools in hydrological modeling as they provide detailed topographical data necessary for analyzing basin characteristics. DEM are utilized to generate key hydrological parameters, including flow direction, flow accumulation, stream networks, and watershed boundaries. In this study, the FABDEM (Forest and Buildings Removed Copernicus DEM), a state-of-the-art dataset available at a 1 arc-second resolution (approximately 30 m), was employed. This dataset, freely accessible through the University of Bristol website, offers refined

elevation data critical for accurate terrain analysis. Alongside the DEM, Land Use Land Cover (LULC) and soil maps were utilized as essential inputs for hydrological modeling using the SWAT model. The LULC map was developed using Landsat 8 satellite imagery at a 30 m resolution, sourced from the USGS Earth Explorer platform. A supervised classification technique, specifically the Maximum Likelihood Classification method, was applied using ERDAS IMAGINE software to categorize the basin into five land cover classes: water bodies, forest, built-up areas, agricultural land, and riverbed/wasteland. Validation of the LULC map was conducted using ground truth data collected via portable GPS devices during field surveys, revealing that 68% of the catchment is forested and 14% is under agricultural use.

The soils property data were obtained from the Harmonized World Soil Database (HWSD) version 1.2, available from the Food and Agriculture Organization (FAO). Based on this data, soils in the basin were classified as clay loam and loam, providing crucial information for modeling soil-water interactions. Additionally, Figure 2 illustrates the hydrological modeling framework of the study area, demonstrating the interaction of inputs such as precipitation and land use with watershed attributes like soil, topography, and river systems. This flow diagram emphasizes how these elements converge to generate outputs such as streamflow and sediment yield, as simulated by the SWAT model, offering an integrated perspective on the hydrological dynamics of the Song River watershed. The thematic maps for Song river catchment are shown in Figure 3.

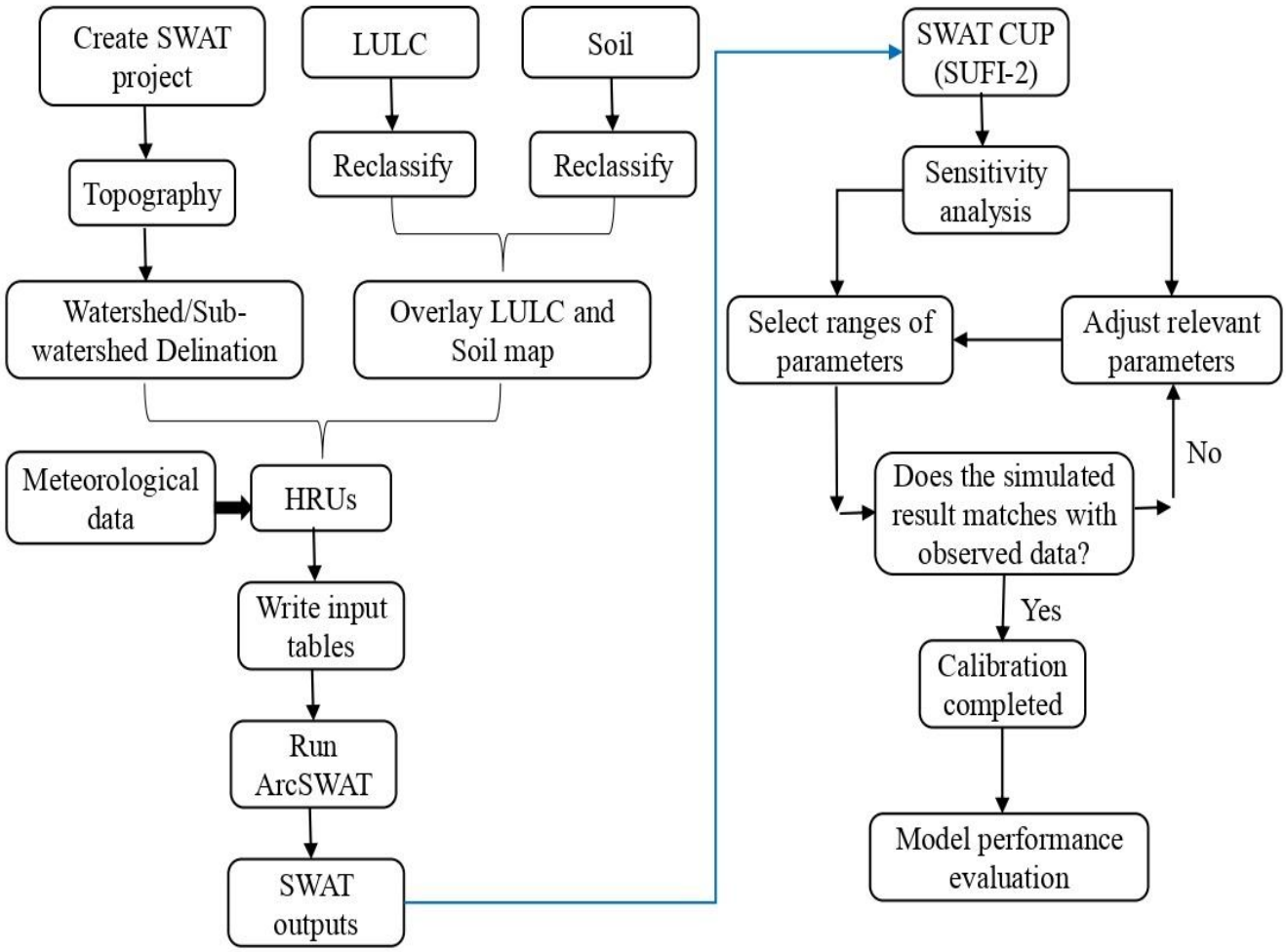

Figure 2: Flow diagram emphasizing the essential elements and processes involved in the hydrological modelling for the study area

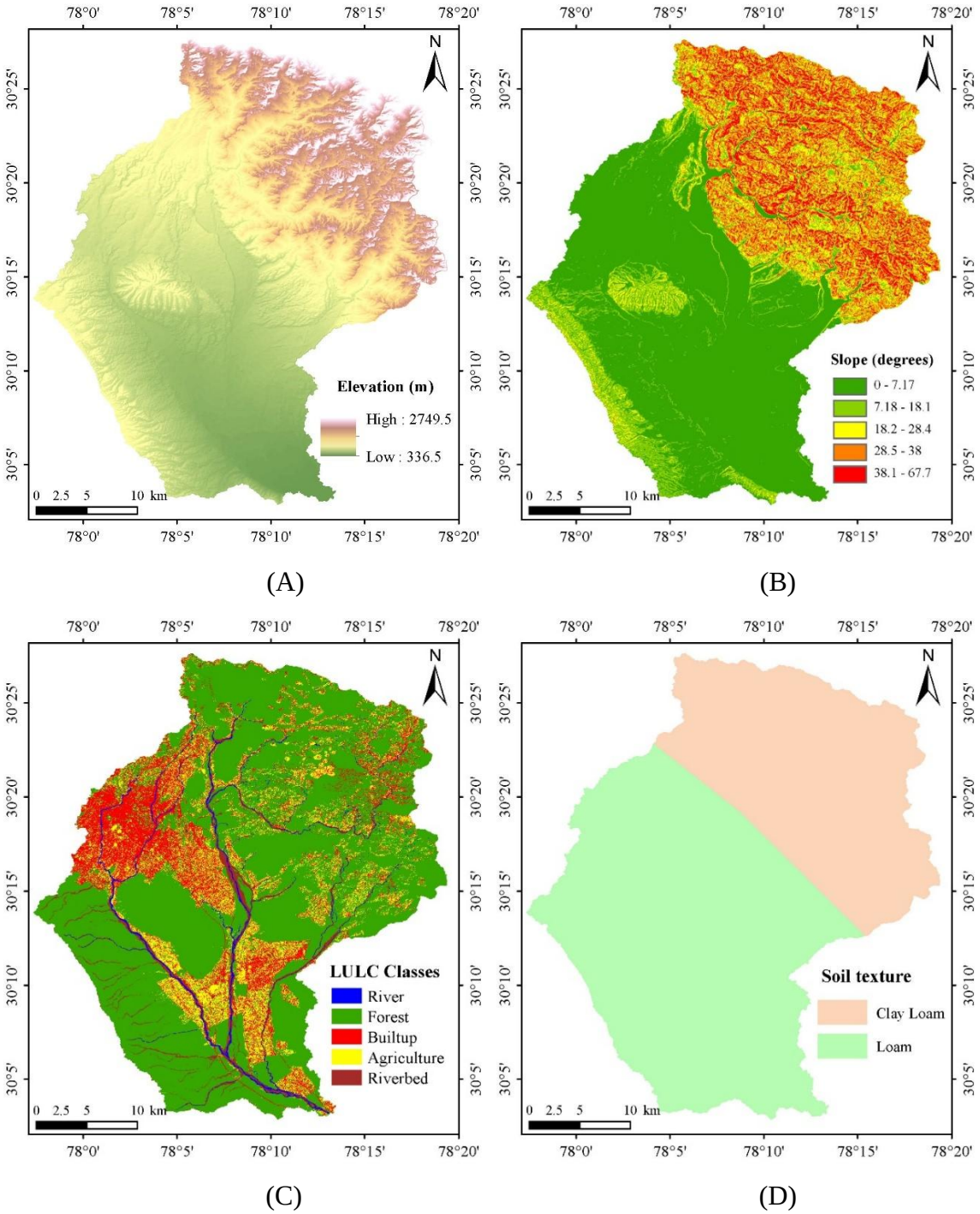

Figure 3: (A) Digital Elevation Model (DEM) map; (B) Slope map; (C) Land cover map; (D) Soil map used as topographical and spatial input for SWAT model

3.4.2 Hydro-meteorological Database

In hydrological modeling, precipitation and air temperature are the fundamental meteorological datasets required for model setup. This study utilized gridded precipitation and minimum and maximum air temperature data on a daily scale, obtained from the India Meteorological Department (IMD), with spatial resolutions of 0.25° x 0.25° and 1° x 1°, respectively.

The observed streamflow data required for calibrating the SWAT hydrological model. The Central Water Commission (CWC), India's central water resource management organization maintained a Gauging and Discharge (GandD) station on the Song River until 2004 at Satyanarayana, located just before the song river's confluence with the Ganga near Rishikesh. For this study, daily streamflow data spanning forty-four years (1971-2004) was obtained from the CWC's Satyanarayana gauging site, designated as site-3. Summary of database used for SWAT model is given in Table 3.

Accurately simulating streamflow and sediment dynamics in recent scenario, a weekly monitoring program was conducted at Site 1 and Site 2 over a period of two monsoon years (June 2022 to November 2023). During this period, weekly discharge measurements were carried out using an Acoustic Doppler Current Profiler (ADCP) instrument to ensure high accuracy. Additionally, one-liter water samples were collected during each site visit for laboratory analysis. Water quality analyses were performed at the National Institute of Hydrology, Roorkee water quality laboratory to determine Total Suspended Solids (TSS) concentrations, expressed in mg/L. These analyses provided critical data for calibrating and validating the suspended sediment component of the SWAT model.

Table 3: Summary of the dataset used in this study

Data set	Source	Scale/Time Series	Data Description/Properties
DEM	FABDEM V1-0	30 m	https://data.bris.ac.uk/data/dataset/25wfy0f9ukoge2gs7a5mqpq2j7
Land cover	Landsat 8	30 m	(https://earthexplorer.usgs.gov/)
Soil	FAO/HWSDv1.2	1:1,000,000	https://www.fao.org/soils-portal/data-hub/soil-maps-and-

			databases/harmonized-world-soil-database-v12/en/
Rainfall (mm)	IMD Gridded	Daily (0.25° x 0.25°)	Rainfall data (1971-2023)
Temperature (°C)	IMD Gridded	Daily (1°x1°)	Max. and Min. temperature (1971-2023)
Discharge	CWC Observed data	Daily / (1971-2004) Weekly / (2022-2023)	CWC Satyanarayana site. Weekly discharge measured using ADCP and FlowTracker2 instrument.
Suspended Sediment	Observed data	Weekly / (2022-2023)	-

3.4.3 Field Survey and Investigation

In the present study, discharge data were available only up to 2004. To address this data gap and validate the model's applicability for recent conditions, river discharge measurements were conducted for more recent periods, specifically 2022-2023. The process of site selection and the methodology employed for discharge measurement are delineated in sections 3.1.4 and 3.1.5. This approach was essential to ensure that the model's predictions remain relevant and accurate for contemporary river conditions, considering potential changes in discharge patterns over time.

3.4.4 Design of Monitoring Programme

The Song River and its primary tributary, the Suswa River, were monitored across two monsoon seasons (June 2022 to November 2023) at two strategically selected sites along the Song River. These stations were situated upstream and downstream of the confluence of the Suswa River, adjacent to road bridges, ensuring accessibility during the monsoon season. Discharge measurements were conducted weekly during the monsoon (June to September), biweekly during the post-monsoon period (October to November), and monthly during the lean seasons (December to May). Table 4 provides details of the monitoring stations.

Table 4: Descriptive characteristics of the selected monitoring stations

Name	Station Code	Sampling Site Location Name	Stream	Latitude (Decimal Degrees)	Longitude (Decimal Degrees)	Elevation (m)
Song U/S	Site-1	Song Bridge, Doiwala	Song	30.17915	78.13162	486.32

Song D/S	Site-2	Song Bridge, Nepali Farm, Raiwala	Song	30.05506	78.21517	346.35

3.4.5 Observed Streamflow and Sediment data

Flow velocity and discharge measurements were conducted using two instruments: the SonTek FlowTracker2 and the Acoustic Doppler current profiler (ADCP). The SonTek FlowTracker2, an Acoustic Doppler Velocimeter (ADV), utilizes the Doppler effect to measure velocities ranging from 0.001 to 4 m/s. For low-flow conditions, the ADV was employed to measure velocity, while the mid-section method was utilized to calculate river discharge. In flood scenarios, a boat-mounted ADCP was deployed to measure both velocity and discharge. The field photographs of discharge measurement using Flow-Tracker2 in low flow condition and using ADCP in high flow condition are shown in Figure 4.

Figure 4: Discharge measurement using (A) Flow-Tracker2 in low flow condition (B) ADCP in high flow condition

Water samples for sediment analysis were collected during each site visit. At all monitoring locations, river water samples were collected using the grab sampling technique. One liter of river water sample was collected in high-density polyethylene (HDPE) containers and transport to the National Institute of Hydrology, Roorkee water quality lab for examination. To ensure uniformity, the collected samples were vigorously agitated. Subsequently, one liter of each sample was filtered through a 0.45-micron gridded cellulose nitrate membrane using an electric vacuum pump to extract suspended sediments. The filter paper containing the captured sediments was then dried in a hot oven to determine the total suspended sediment (TSS) concentration. The TSS concentration in the water sample was calculated by measuring the dry weight difference of the filter paper before and after the filtration process.

3.4.6 Model Setup

The eco-hydrological model Soil and Water Assessment Tool (SWAT) is a versatile hydrological model capable of simulating diverse environmental conditions and scales (Arnold et al., 1998). The establishment of a SWAT model requires spatially distributed data, including Digital Elevation Models (DEMs), soil data, land use land cover maps, and weather data. The model operates exclusively on this data and does not necessitate prior knowledge of catchment behaviour or flow processes. SWAT simulates water balance, a fundamental driver of watershed processes, to accurately predict runoff, sediment, and nutrient movement. The model comprises two primary components: the land phase and the routing phase. For surface runoff estimation, the Curve Number method is utilized.

3.4.7 Model Calibration and Validation and Sensitivity Analysis

The SWAT model encompasses numerous hydrological parameters whose effectiveness is affected by variables such as soil type, slope, and land cover. To identify the most influential parameters and reduce the number needed for calibration, sensitivity analysis is essential. This research employed the SUFI-2 algorithm within the SWAT-CUP interface to perform sensitivity analysis on 13 crucial parameters, including ALPHA_BF (baseflow alpha factor), CH_K2 (hydraulic conductivity in the main channel alluvium), CH_N2 (Manning's "n" for the main channel), as well as GWQMN, SOL_AWC, ESCO, and SURLAG. The impact of these parameters

on hydrological components like discharge, infiltration, baseflow, groundwater flow, evaporation, and transpiration were examined by methodically altering one parameter at a time while keeping others constant. The relationship between parameters and hydrological responses was quantified using sensitivity coefficients. To enhance the model's accuracy, both manual and automated calibration techniques were utilized. Manual calibration involved visually adjusting parameters based on observed and simulated flow patterns, considering catchment characteristics. Automated calibration, facilitated by SWAT-CUP, systematically optimized uncertain parameters by comparing model outputs with measured data through an interactive interface. This combined approach ensured effective parameter optimization and improved the SWAT model's ability to simulate hydrological processes.

3.4.8 Performance Evaluation

There are multiple efficacy measures that can be used to assess the model's performance. These efficacy metrics show how the model-simulated values and the observed values are reconciled. Nash-Sutcliffe Efficiency (NSE), coefficient of determination (R^2) and PBIAS are the most widely utilized metrics among them (Swain et al. 2022).

- **Nash-Sutcliffe efficiency (NSE) (**Nash and Sutcliffe, 1970),

$$\mathrm{NSE} = 1 - \frac{\sum_{i=1}^{n}(O_i - P_i)^2}{\sum_{i=1}^{n}(O_i - \bar{O})^2}$$

- **Percent bias (PBIAS)** (Moriasi *et al.*, 2007),

$$PBIAS = \frac{(\sum_{i=1}^{n}(O_i - P_i) \times 100)}{(\sum_{i=1}^{n} O_i)}$$

- **Coefficient of determination (R^2)** (Suryavanshi *et al.,* 2017),

$$R^2 = \left[\frac{\sum_{i=1}^{n}(O_i + \bar{O})(P_i - \bar{P})}{\sum_{i=1}^{n}(O_i - \bar{O})^2 \sum_{i=1}^{n}(P_i - \bar{P})^2}\right]^2$$

P_i and O_i are the simulated and observed values of discharge; n is the sample number, $\bar{P}$ and $\bar{O}$ are the average of simulated and observed discharge.

CHAPTER - 4
RESULTS AND DISCUSSIONS

4.1 PHYSIO-CHEMICAL CHARACTERISTICS OF RIVER SONG AND TRIBUTARY SUSWA

For better understanding the water chemistry of the river, a comprehensive assessment was conducted on twenty-two physico-chemical water quality parameters at three distinct monitoring stations of the study area depicted in Table 5. The pH of river water at monitoring stations 1, 2, and 3 varies from slightly acidic to slightly alkaline in nature ranging from 5.71 to 8.50; 5.63 to 8.26; and 5.60 to 8.27 respectively with the lowest pH levels were observed during peak monsoon, indicating the addition of low-pH rainwater. The Suswa River exhibited higher EC than the Song River, attributed to untreated sewage influx, with EC values varying from 244 µS/cm to 1038 µS/cm in all three stations. TDS and TSS exhibited extensive temporal fluctuations during monsoon period. The ranges of TDS at station 1, 2 and 3 are 181~768 mg/L, 223~605 mg/L and 260~580 mg/L, with the mean values of 554, 435 and 410 mg/L, respectively. TSS peaked during monsoonal weeks, with station 2 recording values from 142.26 mg/L to 5111.60 mg/L, while station 3 ranged from 129.82 mg/L to 3955.55 mg/L.

The alkalinity of the River Suswa at Station 1 ranged from 89 to 364 mg/L, with a mean value of 261 mg/L. The alkalinity value in the water of the River Song ranged from 91 to 179 mg/L at Station 2 and 111 to 267 mg/L at Station 3. Notably, the maximum alkalinity observed at Station 1 exceeded the criteria limit of 200 mg/L prescribed by the BIS (2012) for drinking water quality.

The hardness levels in the river water at monitoring stations 1, 2, and 3 ranged from 302.90 mg/L to 465.40 mg/L, exceeding the permissible limit of 300 mg/L, primarily due to high calcium concentrations linked to anthropogenic activities (Joshi et al., 2009). This increase in calcium content may be due the amalgamation of anthropogenic activities such as domestic effluents, urban runoff and industrial wastewater (Singh et al., 2005; Khadse et al., 2008; Suthar et al., 2010). However, during the week days of July and August month, the NH_4^+ concentrations exceeded the permissible limit, ranging from 0.27 mg/L to 4.50 mg/L at station 1, 0.09 mg/L to 1.75 mg/L at

station 2, and 0.10 mg/L to 2.19 mg/L at station 3, indicating the aerobic or anaerobic decomposition of organic matter and the mixing of sewage into the river water (Suthar et al., 2010; Groeschke et al., 2017).

DO concentration serves as the primary indicator of river water quality, while the concentration of COD and BOD are both studied to assess the degree of pollution in river water. The DO level in the Song River shows seasonal fluctuations, ranged from 6.00 to 10.94 mg/L at station 2 and 5.79 to 10.84 mg/L at the station 3; with higher values during the post-monsoon and winter months, followed by a gradual decrease during the monsoon season. The concentration of DO in the Suswa River ranged from 4.38 to 9.60 mg/L at the station1. Minimum DO was observed at station 1(4.38 mg/L) below the minimum criteria of 5 mg/L prescribed by CPCB standard. In this study BOD concentration ranging from 2.2 to 16.0 mg/L at station 1, 0.32 to 7.5 mg/L and at station 2 and 0.38 to 12.5 mg/L at station 3, with peak value recorded during rainy season (Sanap et al., 2006). COD ranged from 2.88 mg/L to 51.00 mg/L across all the three stations follows a similar trend, with the highest concentration observed during the monsoon season due to increase organic and inorganic loads.

Table 5: Summary of water quality parameters at the Suswa River and upstream and downstream of the Song River

Parameters	Criteria Limit	Tributary Suswa				River Song Upstream				River Song Downstream			
	BIS acceptable limits (2012)	Min.	Max.	Mean	SD	Min.	Max.	Mean	SD	Min.	Max.	Mean	SD
pH,	6.5 – 8.5	5.71	8.5	7.04	0.68	5.63	8.26	6.97	0.71	5.6	8.27	6.91	0.67
EC, µS/cm	–	244	1038	749	181.72	302	817	587	108.7	352	784	554	101.25
TDS, mg/L	< 500	181	768	554	197.18	223	605	435	80.46	260	580	410	75.12
TSS, mg/L	–	0.8	4405	145	636.94	0.34	5112	354	825.7	1.44	3956	287	621.72
DO, mg/L	$\geq 5^{*}$	4.38	9.6	6.96	1.16	6	10.94	8.11	1.17	5.79	10.84	8	1.13
BOD, mg/L	$\leq 3^{*}$	2.2	16	6.37	3.18	0.32	7.5	2.95	2.24	0.38	12.5	3.8	2.49
COD, mg/L*	$< 10^{*}$	7.2	56	25.9	14.01	2.88	46.8	14.26	10.13	4.2	41.76	14.3	8.11
Alk., mg/L	< 200	89	364	261	58.74	91	179	148	20.27	111	267	174	30.29
Hard., mg/L	< 200	108	465	351	80.3	157	428	302	58.24	176	378	275	55.02
Na^{+}, mg/L	–	3.33	28.6	17.8	5.67	2.29	6.99	4.3	1.03	3.8	10.34	6.83	1.34
K^{+}, mg/L	–	3.51	12.8	6.74	2.14	1.13	2.83	1.96	0.37	1.28	7.55	2.43	0.87
Ca^{2+}, mg/L	< 75	30.7	117	87.3	19.39	38	106	72.4	13.86	42.33	93.9	67.9	13.15
Mg^{2+}, mg/L	< 30	7.69	45.2	32.4	8.11	15	52.12	29.49	6.58	16.19	35	25.8	5.68
HCO_3^{-}, mg/L	–	109	444	318	71.66	111	218.8	180.12	24.73	135.93	326	212	36.95
Cl^{-}, mg/L	< 250	2.79	40.3	21.8	9.06	0.87	5.64	2.28	0.96	2.11	9.39	4.84	2.02
SO_4^{2-}, mg/L	< 200	18.4	128	63.4	17.73	49.1	229.7	136.3	42.17	35.08	126.6	82.4	22.48
NO_3^{-}, mg/L	< 45	0.06	25.6	11.61	6.06	1.22	7.88	5.14	1.4	3.54	10.81	6.57	1.42
F^{-}, mg/L	< 1	0.08	0.23	0.16	0.03	0.06	0.24	0.15	0.03	0.08	1.1	0.17	0.13
NO_2^{-}, mg/L	< 10	0.03	8.79	1.52	1.89	0.02	1.01	0.09	0.19	0.03	0.99	0.11	0.18
NH_4^{+}, mg/L	< 0.5	0.27	4.5	1.43	1.09	0.09	1.75	0.47	0.44	0.10	2.19	0.56	0.48
PO_4^{3-}, mg/L	< 0.1	0.03	4.88	0.87	1.09	0.03	0.34	0.04	0.08	0.02	10.32	0.44	1.56
NICB%	–	-0.11	7.31	3.82	–	-5.37	5.96	2.59	–	-3.56	6.11	3.63	–

***Alk.* alkalinity, *Hard.* hardness, *SD* standard deviation, *NICB* normalized inorganic charge balance**

***Denotes CPCB limits for designated best use for outdoor bathing**

The longitudinal variations of anions and cations at the monitoring stations are presented in Figure 5. The relative monthly average abundance of major cations and anions were found to be in the decreasing order of Ca^{2+}> Mg^{2+}> Na^{+}> K^{+}; HCO_3^{-}> SO_4^{2-}> NO_3^{-} > Cl^{-} at station 2, Ca^{2+}> Mg^{2+}> Na^{+}> K^{+}; HCO_3^{-}> SO_4^{2-}> Cl^{-}> NO_3^{-} at stations 1 and station 3. A similar trend was observed by Sharma et al. (2021). The concentration of major cations and anions presented in Table 3. Among cations, Ca^{2+} ion is the dominant species at all sampling point, contributing 54.80% at station 1, 57.10% at station 2, and 57.73% at station 3.

Among anions, bicarbonate (HCO_3^{-}%) dominates, with the highest proportion at Station 1 (71.00%), followed by Station 3 (64.44%) and Station 2 (48.94%), reflecting carbonate weathering processes. Sulphate (SO_4%) varies considerably, being highest at Station 2 (48.53%), suggesting possible anthropogenic or geological influences. Chloride (Cl%) and nitrate (NO_3%) remain comparatively lower, with Cl% peaking at Sta-1 (8.74%) and declining at Sta-2 (1.14%) and Sta-3 (2.66%), while NO_3% exhibits minimal variations (ranging from 1.40% to 2.72%).

In Suswa River (Station 1), HCO_3^{-} contribute more than 70% of the total anion (TZ^{-}) while 87.9% of the total cation were contribute by (Ca^{2+} + Mg^{2+}). The most dominant ion was Ca^{2+}, which is said to have contributed approximately 68% of the total cation charge (TZ^{+}), followed by Mg^{2+} (15%), Na^{+} (8%) and K^{+} (7%).

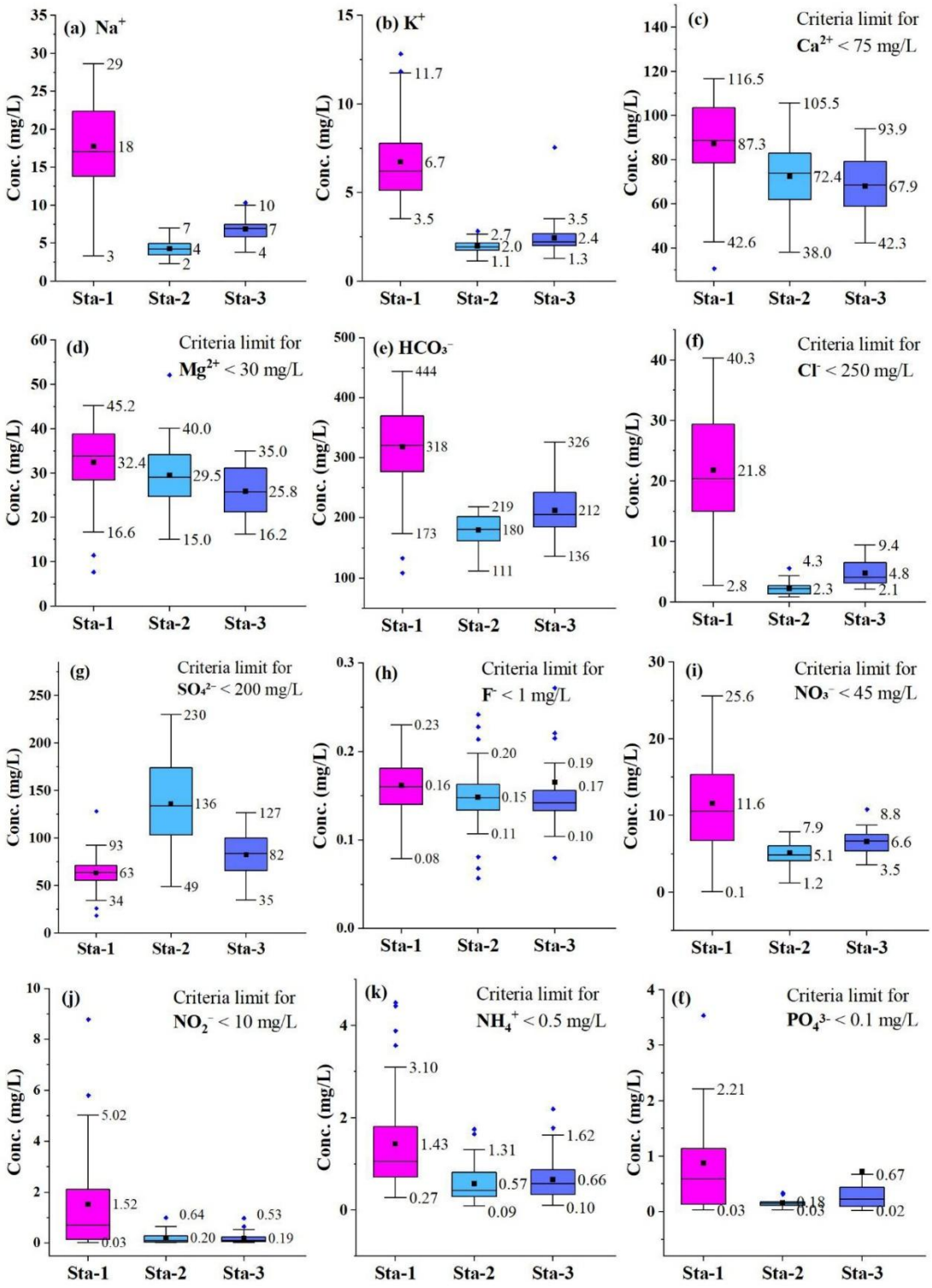

Figure 5: Longitudinal variation of cations and anions at stations 1, 2 and 3. The concentrations are evaluated against the acceptable criteria limit set by BIS (BIS, 2012) for drinking of selected parameters as shown.

High solute concentrations in the Suswa River during dry seasons render it unsuitable for irrigation. EC decreased after the first flush during heavy rainfall in August but increased in

the post-monsoon due to base flow contributions. Elevated TSS levels were linked to precipitation events that transport sediments and agitate particulate matter, contributing to higher concentrations (Jindal and Sharma, 2011). High concentrations of various parameters may be due to high runoff, sewage discharge, and organic material decomposition (Panda et al., 2018). Overall, the study revealed high TSS and COD levels during monsoon months, which may dilute other substances and reduce biological activity, impacting nutrient concentrations in the river.

The time series comparison of pollutant concentrations between the Suswa and Song Rivers at various sampling points, revealing significant differences (Figure 6). The Song River experiences higher concentrations during the rainy season, likely due to runoff and agricultural activities, while the Suswa River maintains more stable levels year-round, indicating less land use impact. This highlights the necessity for targeted water quality management strategies in both rivers, especially where concentration spikes may pose ecological and health risks. All cations (Na^+, K^+, Ca^{2+}, Mg^{2+}, NH_4^+) and anions (HCO_3^-, SO_4^{2-}, Cl^-, NO_3^-, PO_4^{3-}) decrease during the monsoon and peaking during the summer, reflecting dilution from runoff. Nitrate concentrations ranged from 0.06 mg/L to 25.6 mg/L in in winter due to lateral flow and leaching.

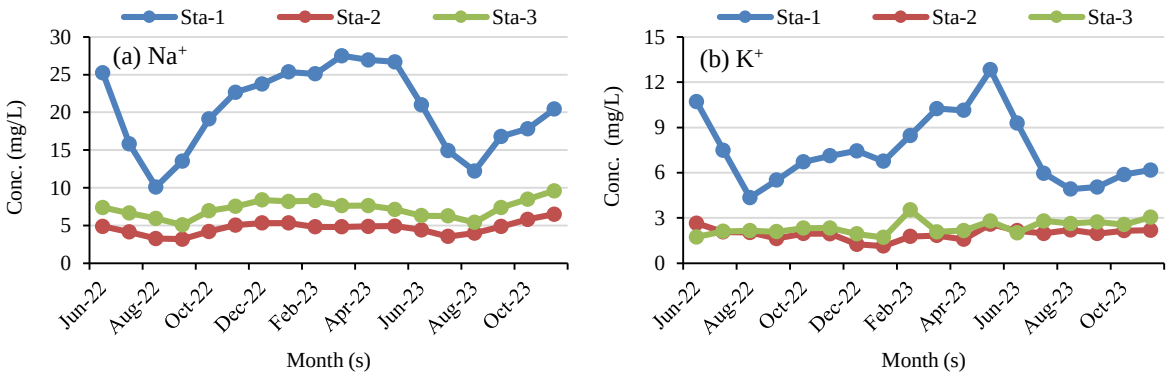

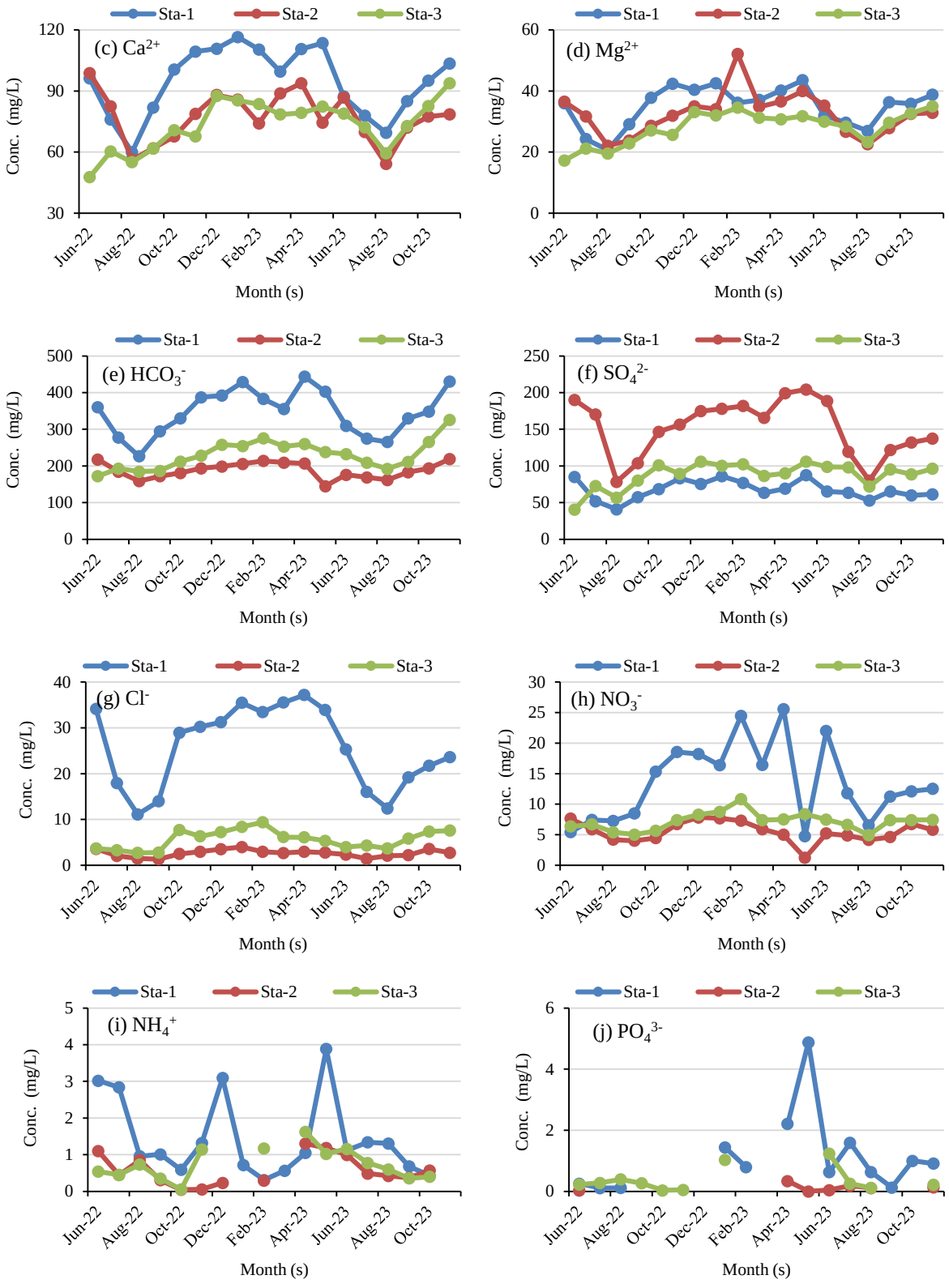

Figure 6: Temporal variation of major anions and cations in the river water of Suswa and Song Rivers

4.1.1 Sources and Governing Mechanism of Riverine Solutes

The Gibbs diagram was proposed a hypothesis to elucidate the primary natural processes influencing the hydrochemistry of the river system, specifically evaporation, rock weathering, and precipitation dominance (Gibbs, 1970). As depicted in Figure 7, the river water exhibits moderate TDS levels and low $Na^+/(Na^+ + Ca^{2+})$ ratios (0.17 for Suswa, 0.06 for Song U/S, and 0.17 for Song D/S) as well as low $Cl^-/(Cl^- + HCO_3^-)$ ratios (0.06 for Suswa, 0.01 for Song U/S, and 0.02 for Song D/S). These values indicate that geological factors and rock weathering predominantly govern the river's hydrochemistry. However, a few samples deviated from this zone due to high TDS concentrations, indicating the influence of anthropogenic activities responsible for the chemical composition of surface water in the study area.

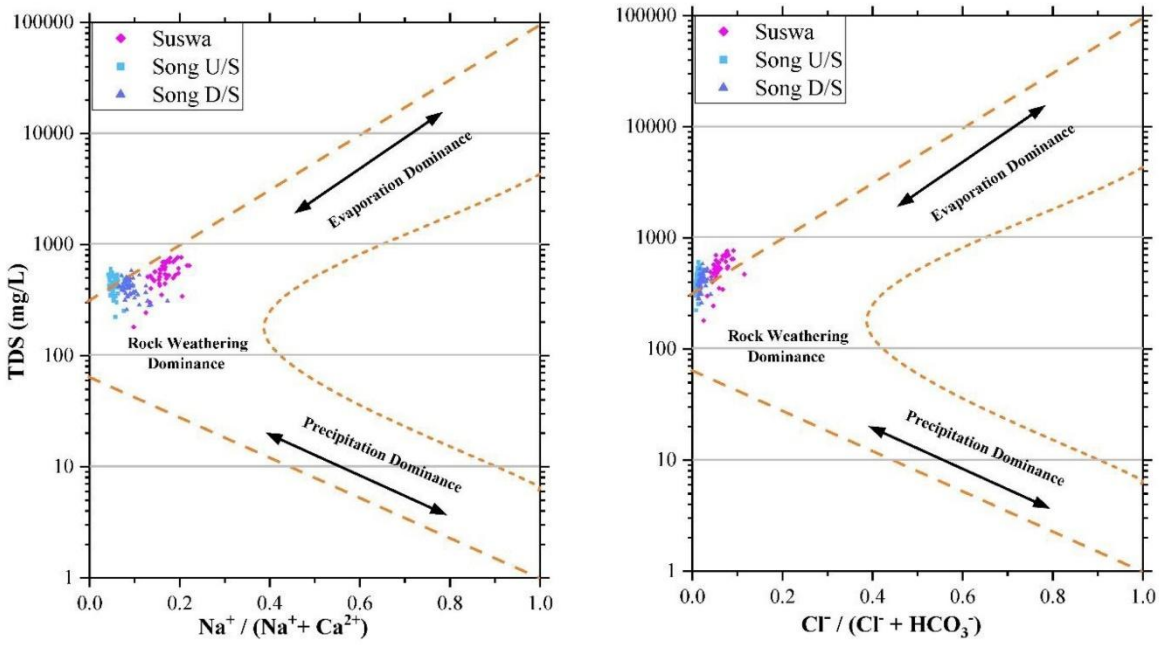

Figure 7: Gibbs plot diagram for Suswa and Song Rivers

The C-ratio is used to assess the relative contributions of two key proton-producing reactions in natural waters: carbonation and sulphide oxidation can be calculated based on the $[HCO_3^-/(HCO_3^- + SO_4^{2-})]$ (Bhanot et al., 2024; Brown et al., 1996). These reactions play a significant role in controlling the acidity and alkalinity of river water. Carbonation refers to the reaction between carbon dioxide and water, producing bicarbonate ions This process is a key source of protons, especially in waters with a high content of carbonates, such as those found in limestone-rich regions. Sulphide oxidation refers to the chemical oxidation of sulphides,

commonly from minerals such as pyrite (FeS_2), which produces sulphate ions (SO_4^{2-}) and protons, contributing to the acidification of water.

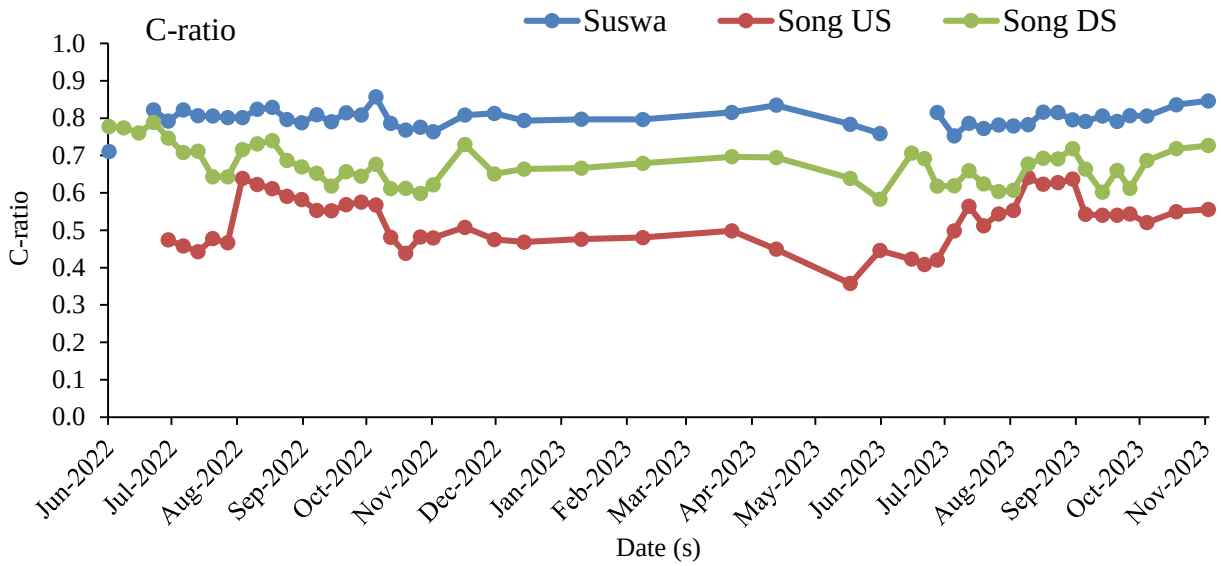

Figure 8: C-ratio of the Suswa and Song Rivers

The value of C-ratio lies between 0 to 1. C-ratio of the Suswa River at station 1 fluctuating between 0.70 and 0.90 throughout the year (Figure 8), suggested that carbonation (bicarbonate formation) is the dominant proton-producing reaction in the system, indicating acid hydrolysis in the water. The average C ratio of Song River at station 2 approximately 0.5 exhibited that coupled reactions involving protons derived from the reaction of sulphide oxidation and carbonate weathering.

4.1.2 Concentration–Flow Relationship

Rainfall runoff data analysis reveals the river Song catchment's heavily dependence on monsoonal precipitation, which constitutes a significant portion of annual rainfall. Figure 9 compares rainfall and discharge plot across all three monitoring stations, captures two monsoon seasons highlighting significant changes in flow patterns. Discharge monitoring revealed that the Suswa River's flow (at Station 1) ranged from 0.13 m^3/s to 16.05 m^3/s, significantly lower than the Song River's upstream (at Station 2) maximum flow of 143.15 m^3/s during the monsoon. The flow of the Song River at downstream (Station 3) varied from 7.09 m^3/s to 201.70 m^3/s, indicating the river's substantial capacity to manage increased runoff during peak rainfall periods. While the Suswa River has sufficient flow during all the seasons to join the Song River, but, the Song River upto its confluence with Suswa River flows mostly below the

surface during the leanest period. Hence, Station 2 becomes dry occasionally during the leanest period.

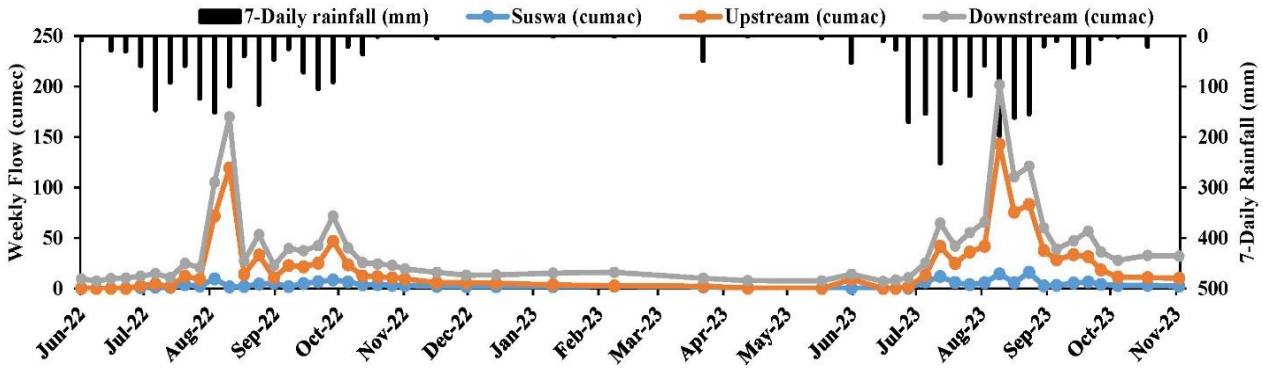

Figure 9: Rainfall vs discharge comparison during the two-consecutive monsoon periods (2022 – 2023)

Temporal analysis of water quality parameters is widely utilised for exploring the dynamics associated to river ion sources. Concentration-flow relationships of ion constituents have been effectively applied in recent years to assess the relative chemical contributions to the river from regular inputs, particularly those influenced by monsoonal rainfall (Bowes et al. 2015). From the correlation between ion concentrations and discharge across various monitoring stations showing a clear inverse correlation between discharge and ion concentration. It can be concluded that the concentration of most of the constituents exhibited a dilution of concentration with the increasing river discharge (Figure 10). It can be inferred from all these plots that the majority of all the chemical constituents exhibit an optimal logarithmic correlation (negative slope) with the flow. However, few exceptions (K^+ and PO_4^{3-} ion at station 3) are exhibited positive slope. A significant correlation was observed Na^+ ($r^2 = 0.41$), K^+ ($r^2 = 0.41$) and Cl^- ($r^2 = 0.41$) at station 1, Na^+ ($r^2 = 0.35$), Ca^{2+} ($r^2 = 0.39$), Mg^{2+} ($r^2 = 0.52$) and Mg^{2+} ($r^2 = 0.63$) at station 2 while station 3 shows Na^+ ($r^2 = 0.45$), Ca^{2+} ($r^2 = 0.47$), Mg^{2+} ($r^2 = 0.41$) and SO_4^{2+} ($r^2 = 0.31$). K^+ and Cl^- ion demonstrated a good correlation in the Suswa River flow (station 1), whereas their correlation was relatively weak in the Song River (station 2 and 3).

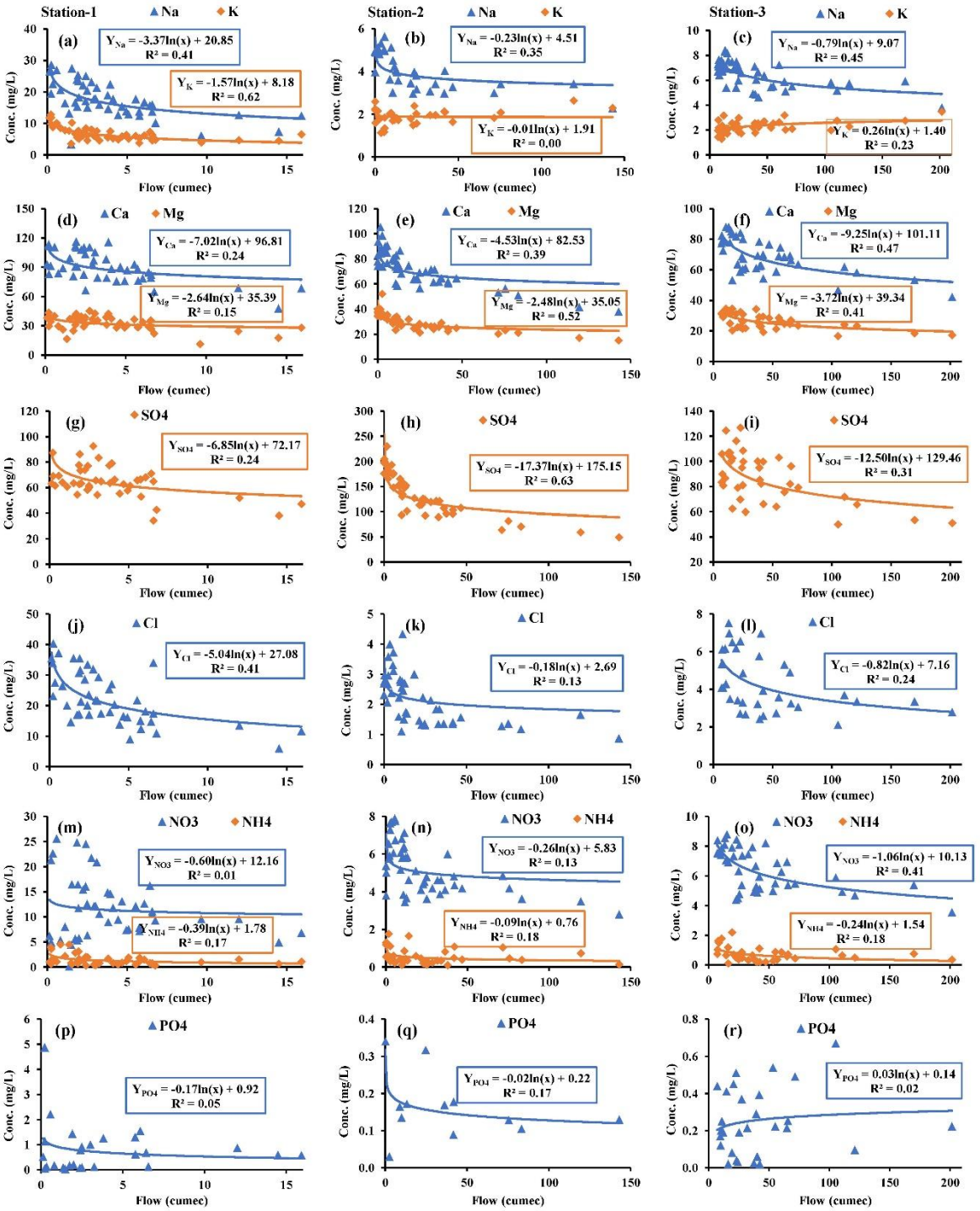

Figure 10: Relationship between flow and major ion concentration in the river water at station 1, 2 and 3 respectively

4.2 ASSESSMENT OF POLLUTANT LOADS

4.2.1 Chemical Mass Balance Approach

The above described CMB approach has been effectively applied in the preset study to assess the contribution of non-point sources of pollution to river Song. The mass loadings of water quality constituents at the upstream and downstream stations may be utilized in the mass balance approach to assess the NPS contribution into the river system. The appearance of NPS pollution inputs as inferred from the study represents that there ought to be some small point sources of pollution which remain unmarked in the course of study. The additional inputs required to balance the chemical mass approach are explained by the factors such as non-point sources of pollution due to agricultural practices, groundwater interference, remobilization of contaminated sediments or a combination of these resources (Angello et al., 2020; Sharma et al., 2021).

4.2.2 Point Source Loadings

Station 1 corresponds to the river Suswa confluencing the Song River in between the 21 km upstream (Station 2) and downstream (Stations 3) monitoring stretch was treated as point source as it carries municipal sewage of Dehradun city through the Rispana and Bindal drainage networks as well as the waste water of Doiwala city from several small scale nalas (CPCB, 2019; Pandey et al., 2021). The major contribution of point source input load for Na^{+}, K^{+}, Ca^{2+}, Mg^{2+}, Cl^{-}, SO_4^{2-}, NO_3^{-}, NH_4^{+}, PO_4^{3-} and HCO_3^{-} to the Song River was observed during monsoon periods were estimated using equation (1) are depicted in Table 5. The loading at station 1 is very less due to flow at this station is low.

4.2.3 Differential Loadings

To assess changes in pollution load in the river stretch during the monitored period, differential loading (upstream-downstream approach) provides a comparison of pollution loads between two monitoring stations, which reflects the cumulative effect of all inputs (point and non-point sources) and processes that occur between the two points (upstream-downstream). A similar approach was also followed by Angello et al., 2020; Sharma et al., 2021.

4.2.4 Estimation of Non-point Source Loadings using Chemical Mass Balance Approach

Uncharacterized loading reflects the pollution loads that come from diffused sources which cannot be easily traced and quantify. CMB approach has been successfully applied to calculate uncharacterised loads from various sources such as urban runoff, agricultural practices, groundwater interactions, or sediment contributions at the catchment outlet (Station 3). The uncharacterised loads in 21 km stretch of the Song River, covering a catchment area of 305 sq. km include approximately 14% agricultural land and 71% forest area (Quamar et al., 2025). Suswa River joining the Song River between the monitoring stretch was treated as point source as it carries municipal sewage of Dehradun city through the Rispana and Bindal drainage networks as well as the waste water of Doiwala city from several small scale nalas (CPCB, 2019; Pandey et al., 2021). Therefore, the difference between estimated differential loadings and point sources loadings may be caused by the contribution of uncharacterized non-point sources of pollution due to urban runoff, agricultural practices, groundwater interactions, or sediment transport contributions.

The input fluxes from the tributaries within the selected reach, along with upstream input fluxes and downstream output fluxes are typically calculated from rigorous monitoring of discharge measurements and periodic water quality analysis at strategically selected stations for different constituents.

The loadings from uncharacterized sources for different constituents in Song River has been depicted in the Figure 11. The contributions of uncharacterised non-point sources of pollution possibly may be attributed from the variance in estimating point source loadings and differential loading due to underground water contribution, cultivation practices, sediment water interactions and some unnoticed point sources of pollution (Sharma et al., 2021).

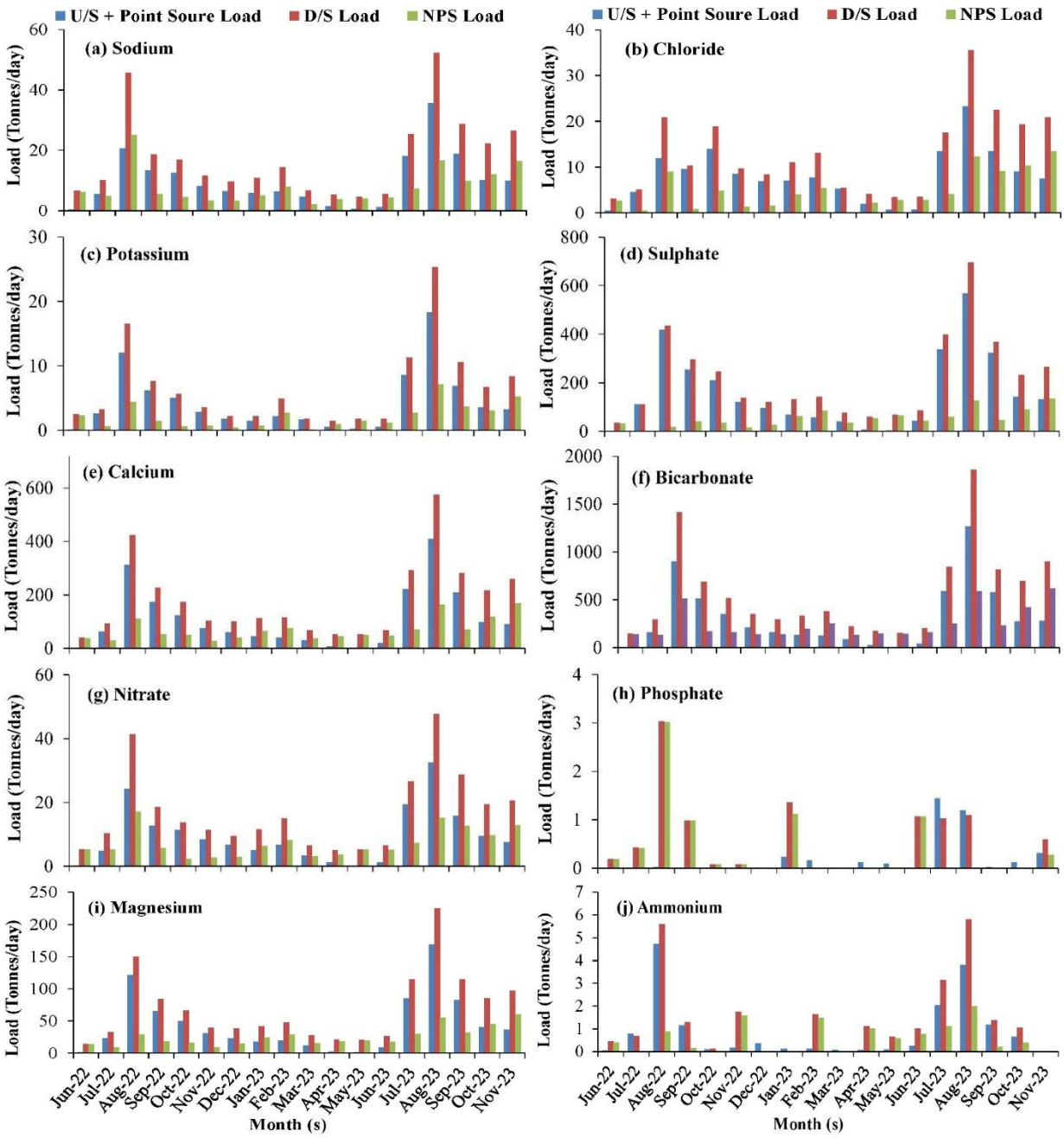

Figure 11: Loadings of Uncharacterized sources to the Song River catchment for various constituents

The contribution of uncharacterized pollution sources at the downstream (Station 3) fluctuates monthly as depicted in Table 6. Contributions remains high during the dry month (April-June) and they decrease significantly during the monsoon season (July–September). Na^+, K^+ and NO_3^- contribution from uncharacterised sources is maximum in June while minimum in July. K^+ showed the lowest contribution from uncharacterised sources in March 2023 (6.12%) and peaked in June 2023 (86.46%). Ca^{2+} contribution from uncharacterised sources is minimum in September 2023 (25.70%) and maximum in May 2023 (94.70%), while Mg^{2+} followed a similar

trend with the lowest contribution in August 2022 (26.16%) and the highest in May 2023 (94.25%). The contribution of Cl^- from uncharacterized sources was minimum in September 2022 (8.31%) and maximum in June 2023 (87.77%). SO_4^{2-} was lowest in July 2022 (8.60%) and peaked in May 2023 (94.95%). NO_3^- exhibited the lowest contribution in October 2022 (19.83%) and the highest in May 2023 (98.12%). PO_4^{3-} showed exceptionally high contributions in August 2022 (99.50%), exhibited an external source, while some months shows a negative value, possible due to losses or sampling uncertainties.

Table 6: Monthly variation of uncharacterized sources of pollution loads

Month	Na^+ %	K^+ %	Ca^{2+} %	Mg^{2+} %	Cl^- %	SO_4^{2-} %	NO_3^- %	NH_4^+ %	PO_4^{3-} %	HCO_3^- %
Jun-22	88.76	82.93	82.77	82.64	70.59	67.42	90.63	67.62	96.78	87.61
Jul-22	44.65	16.07	33.16	30.39	11.25	8.60	50.28	-1.53	95.22	45.42
Aug-22	53.57	27.29	33.55	26.16	47.15	14.98	44.20	26.16	99.50	42.21
Sep-22	29.99	20.68	23.69	21.18	8.31	12.38	29.85	18.50	100.00	23.91
Oct-22	28.03	12.71	30.40	26.34	24.54	17.49	19.83	0.85	100.00	33.11
Nov-22	32.48	23.38	30.28	27.83	18.63	11.86	34.46	1.63	100.00	42.08
Dec-22	33.46	18.99	40.75	39.31	18.64	22.05	30.35	-	-	46.79
Jan-23	45.73	34.67	59.26	58.29	35.64	47.64	55.85	-	82.42	59.81
Feb-23	55.89	55.81	65.77	59.82	41.33	59.92	55.02	91.96	45.53	66.52
Mar-23	31.45	6.12	55.78	57.33	3.40	46.58	48.76	-	-	60.44
Apr-23	72.05	63.27	86.20	86.84	53.60	87.80	72.83	92.86	-	85.03
May-23	87.98	85.16	94.70	94.25	80.51	94.95	98.12	87.22	-	94.17
Jun-23	90.31	86.46	88.66	89.27	87.77	82.13	90.04	90.41	97.03	91.98
Jul-23	30.97	26.24	26.94	28.11	27.78	19.55	29.22	30.70	45.69	31.78
Aug-23	37.15	32.98	29.39	26.63	44.85	20.89	33.00	43.68	70.01	32.93
Sep-23	34.70	35.86	25.70	28.52	40.27	13.24	45.01	17.21	-	28.44
Oct-23	56.59	49.56	55.25	54.46	56.44	39.77	52.57	42.88	-	61.51
Nov-23	62.21	61.81	65.24	61.99	64.27	50.40	62.51	-	47.27	68.70

Comparison of the total pollutant load in the Song River during two monsoon periods (2022 and 2023) exhibited that Na^+, K^+, Ca^{2+} and Mg^{2+} increases 5.71%, 33.41%, 16.86% and 26.20% respectively. While in case of anions, maximum increase in load 51.56% observed for Cl^-, and SO_4^{2-} increases 23.01%, NH_4^+ increases 36.19%, NO_3^- increases 12.36% and HCO_3^- increases 22.61% while PO_4^{3-} decreases (Table 6). In lean period shows that Suswa River flow below the bed surface before confluence with Song River. So, all the PO_4^{3-} does not reach to Song River during lean period. Comparative analysis of rainfall data for the Song River catchment in the year 2022 and 2023, highlighting significant variations in precipitation data. This represents a

16% increase in annual rainfall and a 22% increase during the monsoon period compared to the previous year. The earlier onset of the monsoon in June 2023 contributed to increased rainfall during the early months, although September experienced less precipitation than in 2022.

The contribution of pollutant loads through point sources (PS) and non-point sources (NPS) or uncharacterized sources for various ions to the Song River was estimated using equation (1 and 2) and is summarized in Table 7 as follows:

Table 7: Summary of annual pollutant loads from point and non-point sources

Parameter	Pollutant Loads (tonnes/year)					Percentage	
	Station 1	Station 2	Station 3	Diff. Loadings	NPS Loadings	PS	NPS
Na^+	1310.25	1179.53	4628.41	3448.88	2138.62	37.99	62.01
K^+	475.39	615.40	1573.90	958.50	483.11	49.60	50.40
Ca^{2+}	6497.15	19642.14	45457.38	25815.24	19318.09	25.17	74.83
Mg^{2+}	2320.05	7930.83	16951.55	9020.72	6700.68	25.72	74.28
Cl^-	1686.11	613.48	3341.90	2728.42	1042.31	61.80	38.20
SO_4^{2-}	4465.36	34389.29	54282.36	19893.07	15427.71	22.45	77.55
NO_3^-	959.35	1479.95	4485.70	3005.75	2046.40	31.92	68.08
NH_4^+	73.18	136.65	336.27	199.63	126.44	36.66	63.34
PO_4^{3-}	19.25	0.25	515.59	515.34	496.09	3.74	96.26
HCO_3^-	776.07	3324.42	8152.63	4828.22	4052.15	16.07	83.93

4.3 SWAT MODEL DEVELOPMENT

4.3.1 Calibration, Validation and Sensitivity Analysis

This research utilized previous studies to guide parameter selection for calibration, examining 13 parameters in total, with 8 identified as sensitive at a 0.05 significance level. Table 8 outlines the range, fitted values, t-statistics, significance levels, and sensitivity rankings for these parameters. The study employed a three-year warm-up period (1971–1973), with calibration and validation periods spanning 1974–1995 and 1996–2004, respectively. The dotty plots generated in SWAT-CUP indicate that the baseflow recession constant (ALPHA_BF) and Channel roughness (CH_N2) are the most sensitive parameters. This conclusion is evident from the noticeable variation in the model's performance metrics corresponding to changes in their values. The ALPHA_BF was calibrated to 0.05, suggesting a contribution of groundwater to streamflow, during low-flow periods is a critical factor in accurately simulating streamflow. CH_N2 was set at 0.04, indicative of a dredged channel, while effective hydraulic conductivity

(CH_K2) was calibrated to 121.15 mm/h, signifying high-permeability conditions. The return flow threshold depth (GWQMN) was set at 735 mm, and soil water capacity (SOL_AWC) showed a 47% decrease, indicating reduced plant-available water. The groundwater "revap" coefficient (GW_REVAP) was calibrated to 0.07, suggesting limited water movement to the root zone. Manning's coefficient (OV_N) was determined to be 0.83, and deep aquifer percolation (REVAPM) required 404.5 mm of shallow aquifer water. Soil evaporation compensation (ESCO) was set at 0.12, indicating high demand from lower soil layers. Surface runoff lag time (SURLAG) was calibrated to 2.33, and plant uptake compensation (EPCO) decreased to -0.29, demonstrating reduced uptake in lower soil layers. Groundwater delay (GW-DELAY) was established at 472.5 days, indicating a slow aquifer response, while lateral flow travel time (LAT_TTIME) was set at 22.14 days, representing lateral flow dynamics within the hydrological response units (HRUs). These calibrated parameters significantly enhanced model performance and improved the simulation of hydrological processes.

Table 8: Fitted values of the SWAT parameter and statistics of sensitivity analysis

Parameter Name	Min. value	Max. value	Fitted Value	t-Stat	P-Value	Rank
V__ALPHA_BF.gw	0.0	1.0	0.05	-47.66	0.00	1
V__CH_N2.rte	0.0	0.1	0.04	21.53	0.00	2
V__CH_K2.rte	51.0	127.0	121.15	14.65	0.00	3
V__GWQMN.gw	0.0	5000.0	735.00	-11.80	0.00	4
R__SOL_AWC(..).sol	-0.5	0.2	-0.47	10.31	0.00	5
V__GW_REVAP.gw	0.0	0.2	0.07	-10.30	0.00	6
R__OV_N.hru	0.0	1.0	0.83	3.42	0.00	7
V__REVAPMN.gw	0.0	500.0	404.50	2.10	0.04	8
V__ESCO.bsn	0.0	1.0	0.12	1.25	0.21	9
V__SURLAG.bsn	0.1	24.0	2.33	1.02	0.31	10
R__EPCO.bsn	-0.5	1.0	-0.29	-0.37	0.71	11
V__GW_DELAY.gw	0.0	500.0	472.50	0.33	0.74	12
R__LAT_TTIME.hru	0.0	180.0	22.14	-0.18	0.86	13

4.3.2 Model Performance Evaluation

The study employed daily observations from 1974 to 2004, with Figure 12 illustrating the temporal comparison between observed and simulated discharge during both calibration and validation phases. Model effectiveness was assessed using R^2, NSE, and PBIAS metrics, as presented in Table 9. The observed and simulated flows showed strong correlation, with R^2 values of 0.79 and 0.66 for calibration and validation, respectively. During calibration, both baseflow and peak flows aligned well between observed and simulated data. Although the

validation period showed underestimated goodness of fit, the results remained satisfactory. The NSE reached 0.7 during calibration and 0.62 during validation. PBIAS values fell within acceptable ranges for both periods, measuring 17.06 for calibration and 19.60 for validation.

Table 9: Model performance statistics

Time series	R^2	NSE	PBIAS
Calibration (1974-1995)	0.77	0.70	17.06
Validation (1996-2004)	0.75	0.68	19.60

The weekly average simulated and observed flow for the 1974-2004 period is depicted in Figure 12 as a time series plot. This graph reveals a high degree of similarity between the simulated and observed discharge, with the model successfully capturing overall flow trends, including seasonal fluctuations and high-flow events. The simulated flow closely tracks the observed data during the calibration phase, demonstrating the model's precision in replicating both low-flow conditions and peak discharge occurrences. Although the validation period exhibits minor underestimations of some peak flows, the general trend remains aligned, indicating satisfactory model performance across the extended timeframe. This sustained consistency underscores the model's dependability for long-term hydrological flow simulations.

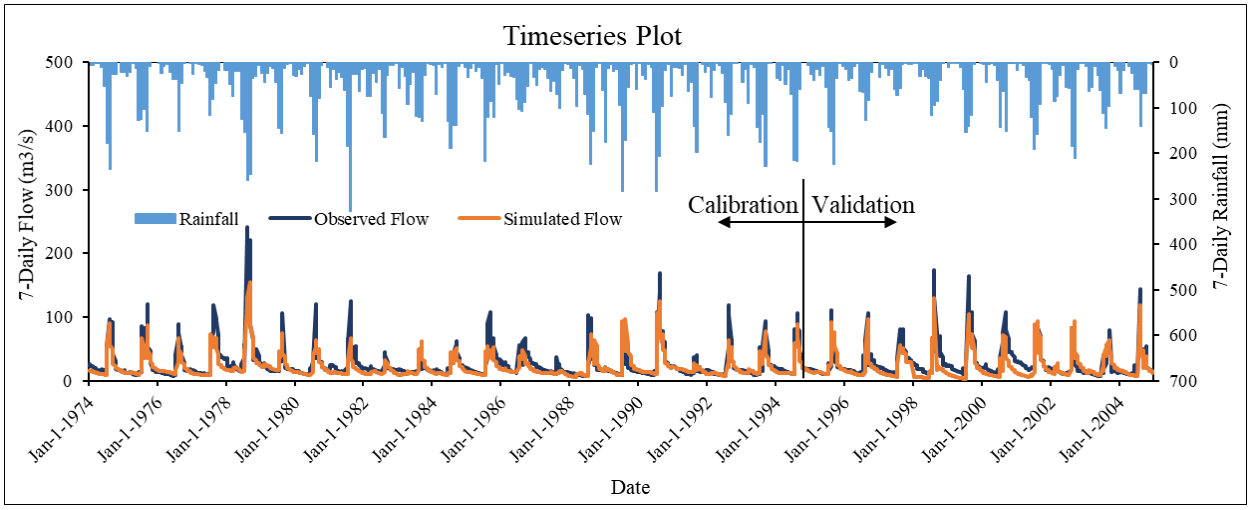

Figure 12: Time series plot of weekly mean observed and simulated flow (1974-2004) at site 2 maintained by CWC

Figure 13 presents a scatter plot depicting the weekly mean simulated versus observed flow during the calibration and validation periods. The plot demonstrates a strong linear relationship between the simulated and observed flow data, with the majority of points clustering in close proximity to the 1:1 line, indicating a high degree of accuracy in the model's predictions. During the calibration period, the scatter plot exhibits a tight correlation, reflecting the model's efficacy in capturing the observed flow dynamics. Although the validation period displays a slight dispersion from the 1:1 line, the overall alignment remains satisfactory, confirming the model's robustness in simulating streamflow across diverse hydrological conditions.

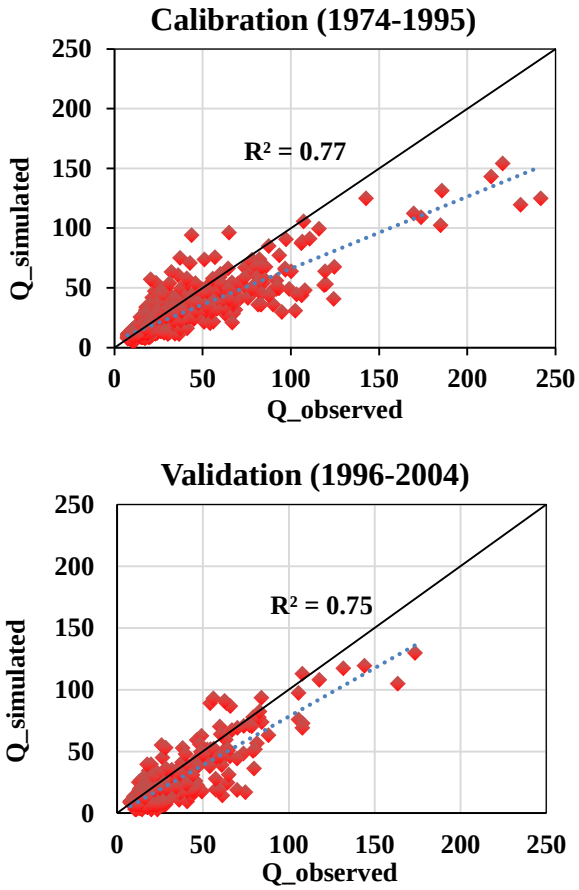

Figure 13: Scatter plot of weekly mean simulated and observed flow during calibration and validation

4.3.3 Model Performance Evaluation with Field Survey Data

The model's applicability to the study area was evaluated by comparing its simulated flows with ADCP-measured discharges obtained during a field survey. A strong correlation was observed between the simulated flows and observed discharge data at both upstream (site-1) and downstream (site-2) locations. The model's performance was quantified using statistical

indicators R^2, NSE, and PBIAS, with results presented in Table 10, demonstrating its robust performance. The R^2 values, ranging from 0.78 to 0.79, indicated a strong correlation, while NSE values of 0.79 upstream and 0.68 downstream showed high agreement between simulated and observed flows. PBIAS values of 0.04 upstream and -16.20 downstream fell within acceptable ranges, further confirming the model's reliability. A time series plot comparing weekly mean simulated flows with observed flows for 2022–2023 at both sites is shown in Figure 14. The plot reveals exceptional alignment at the upstream site, where the model accurately captures flow variations and peak flows. Although minor discrepancies are noted at the downstream site, the overall flow patterns are well-represented, highlighting the model's ability to accurately simulate flow conditions in the Song River basin under diverse field conditions.

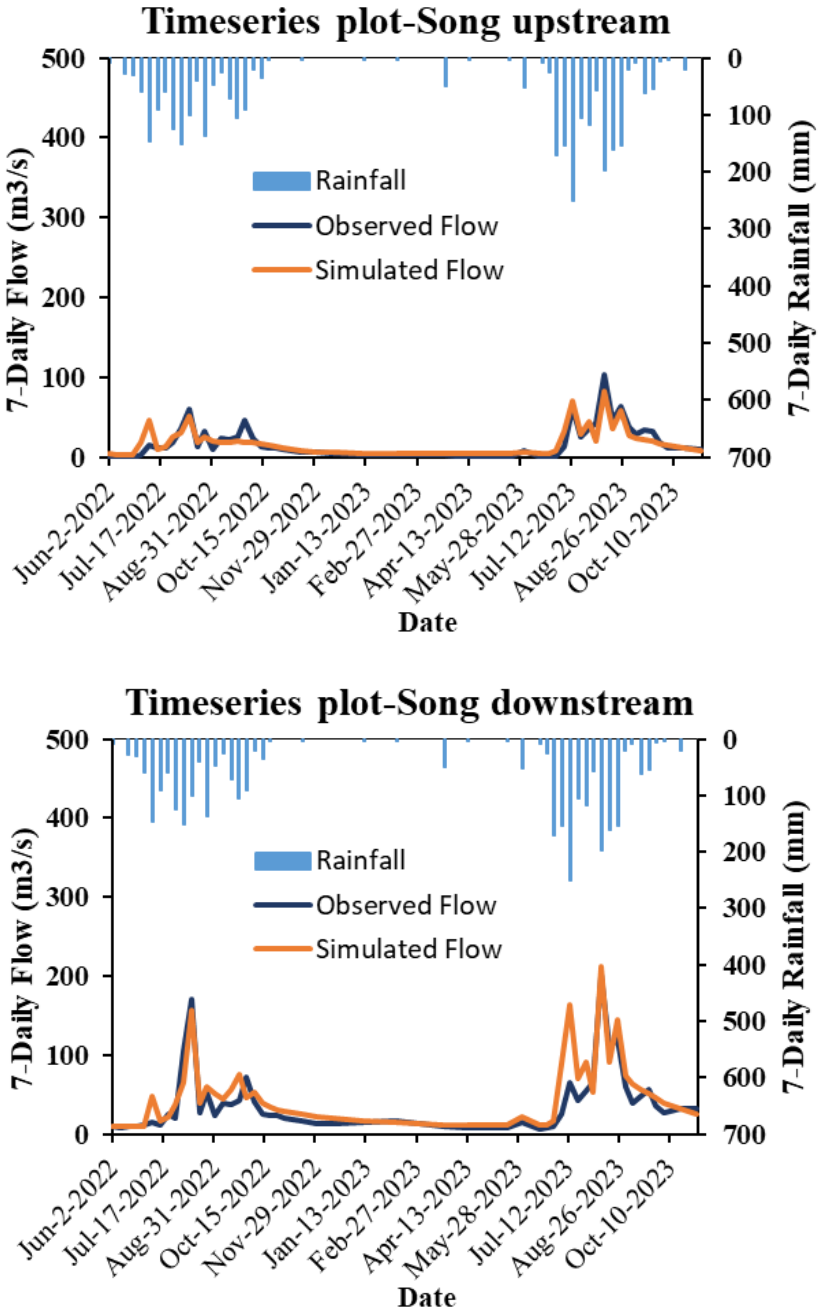

Figure 14: Time series plot of the weekly mean simulated flow and field survey observed flow (2022-2023) at the upstream and downstream sections of the Song River

Figure 15 presents a scatter plot depicting the relationship between weekly mean simulated flow and field survey observed flow at both the upstream and downstream sections of the Song River. The plot demonstrates a strong correlation between the simulated and observed data, with data points closely aligned with the line of perfect agreement. The upstream section exhibits a marginally higher degree of concordance, indicating superior model accuracy in this region, while the downstream section, despite displaying some dispersion, still demonstrates

robust predictive performance. In aggregate, the scatter plot corroborates the model's efficacy in replicating observed flow conditions across distinct sections of the river.

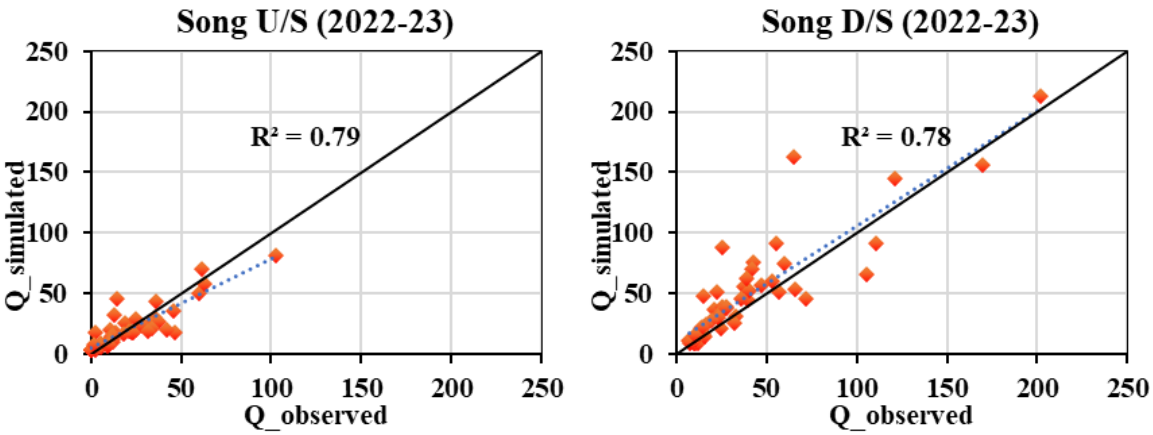

Figure 15: Scatter plot of weekly mean simulated flow and field survey observed flow at upstream and downstream of Song River

Table 10: Performance of calibrated model with field survey data

Sites	Coefficient of Determination (R^2)	NSE	PBIAS
Song Upstream	0.79	0.79	0.04
Song Downstream	0.78	0.68	-16.20

4.3.4 Model Calibration and Validation for Weekly Sediment Load

The pre-calibrated runoff model was subsequently utilized for sediment load calibration. Four additional parameters Channel erodibility factor (CH_EROD), Peak rate adjustment factor for sediment routing in the subbasin (ADJ_PKR), USLE equation support practice (P) factor (USLE_P) and Linear parameter for calculating the maximum amount of sediment (SPCON) added in SWAT-CUP using SUFI2 algorithm for calibrate and validate Sediment load, at daily time scale (Table 11). The results of the best simulation (based on efficacy measures on daily scale) and its comparison with respect to the observed sediment load along with the observed discharge at weekly scale for 2 years i.e., 2023-2024 are presented in Figure 16. The statistical performance indicators for the calibration period (2022) revealed that the model achieved an R^2 value of 0.70 and a Nash-Sutcliffe Efficiency (NSE) of 0.53. For the validation period (2023), the model demonstrated an R^2 of 0.59 and an NSE of 0.52.

Table 11: Fitted values of the SWAT parameter for sediment analysis

Parameter Name	Definition	Min. value	Max. value	Fitted Value
V_CH_EROD.rte	Channel erodibility factor	0.0	0.304	0.007
V_ADJ_PKR.bsn	Peak rate adjustment factor for sediment routing in the subbasin	0.5	1.0	0.79
V_USLE_P.mgt	USLE equation support practice (P) factor	0.6	1.0	0.76
V_SPCON.bsn	Linear parameter for calculating the maximum amount of sediment	0.0001	0.01	0.003

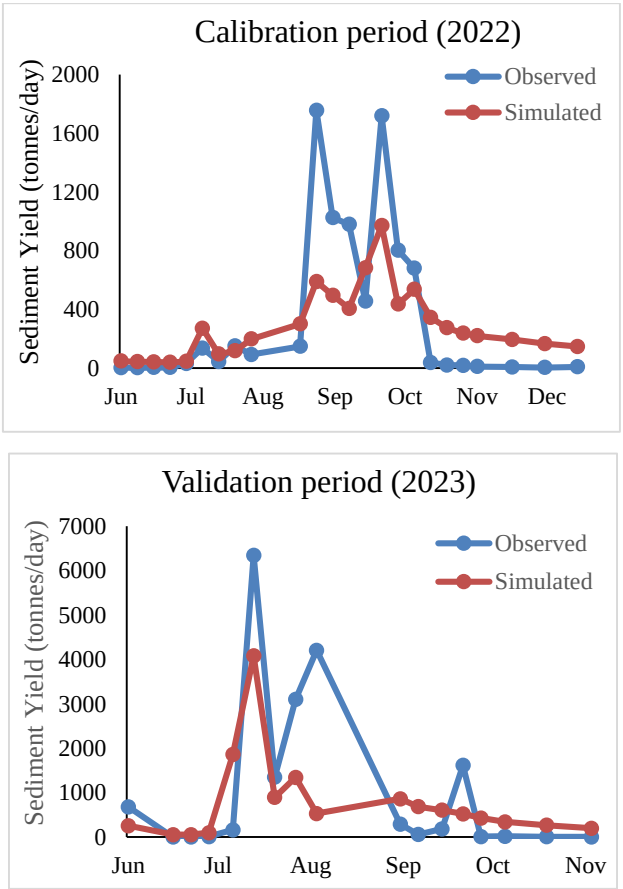

Figure 16: Sediment load calibration and validation plot at Song D/S

Figure 16, comparing observed and simulated daily sediment yields at site 2 during the 2022 calibration and 2023 validation periods, elucidates both the efficacy and limitations of the SWAT model. In the 2022 calibration period, observed sediment yields exhibit substantial peaks in September and October, with loads reaching up to 1,800 tonnes per day. While the SWAT model captures the overall seasonal pattern, including the pronounced increase during the monsoon and subsequent decline, it underestimates the magnitude of these peaks,

particularly during high-flow events. Similarly, during the 2023 validation period, the observed sediment yield peaks in July, exceeding 6,000 tonnes per day, followed by a rapid decline and smaller peaks in subsequent months. The simulated sediment yield generally follows this trend but significantly underestimates the July peak, reaching only approximately 4,000 tonnes per day, and fails to capture some of the acute fluctuations observed in the following months. These results demonstrate the model's capacity to replicate the general seasonal dynamics of sediment transport but also underscore challenges in accurately simulating extreme events. To enhance the model's performance, particularly during high-flow periods, further refinement of parameters or the incorporation of additional factors may be necessary.

CHAPTER – 5
CONCLUSIONS

The present study investigated the hydrogeochemical characteristics of the Song River primarily influenced by rock weathering, anthropogenic activities, with minor contributions from atmospheric inputs. In the Song River catchment, bicarbonate and sulphate are the dominant anions, while calcium and magnesium are the primary cations, reflecting the significant role of carbonate and sulphide oxidation processes. The observed spatiotemporal monitoring data at various upstream and downstream station concludes a strong seasonal dependency of ion chemistry. The major ion composition of most of the water quality parameters are following an inverse relationship with flow, following a logarithmic trend, while chemical loading or fluxes increased with discharge. The chemical mass balance approach was successfully used to estimate the non-point sources of pollutions, revealing potential contributions from agricultural runoff, groundwater interactions, and unidentified point sources. This simplified approach benefits a cost-effective alternative for understanding the impact of non-point source pollution on river water quality. The results of this could be utilized for the management of the catchment, thereby ensuring the long-term health of the riverine ecosystem.

Overall, the study emphasizes the intricate interplay between hydrological processes and human activities in determining the water quality of the river Song. Continuous monitoring and targeted management strategies are essential to safeguard its water quality and mitigate downstream impacts on the river Ganga, thereby ensuring the long-term health of the riverine ecosystem.

The present study demonstrates the efficacy of the SWAT model in simulating streamflow and sediment yield within the Song River watershed, establishing its reliability for hydrological modelling in comparable basins. A comprehensive runoff calibration and validation process refined 13 critical parameters, with 8 identified as highly sensitive, significantly enhancing the model's accuracy. During the calibration phase (1974-1995), the model achieved an R^2 of 0.79 and a NSE of 0.70, indicating a robust correlation between simulated and observed discharge capture both baseflow and peak flow dynamics with high precision. Although a slight decrease in performance occurred during the validation period (1996-2004), with R^2 and NSE values of

0.66 and 0.62, demonstrating its robustness across varying conditions suggesting the model maintains efficacy under changing conditions, such as alterations in land use and climate. The Percent Bias (PBIAS) values of 17.06% during calibration and 19.60% during validation indicated underestimate the model. Furthermore, real-time observed field data from 2022-2023 reinforced the model's accuracy, with strong correlations (R^2 = 0.79 upstream and 0.78 downstream), validating its applicability for watershed management and planning.

In addition to streamflow, the model was evaluated for sediment transport, successfully capturing seasonal trends in sediment dynamics. The R^2 and NSE value for weekly sediment yield at site 2 was obtained as 0.70 and 0.53 respectively for the calibration period and 0.59 and 0.52 respectively for the validation period. However, the model underestimated sediment yields at site 2 during high-flow events, indicating the necessity for further refinement to enhance predictions under extreme weather conditions, such as floods. Notwithstanding this limitation, the model's capability to simulate sediment transport remains valuable for comprehending sediment dynamics and addressing sediment-related issues in watershed management.

The calibration and validation results indicate that the model performs well in simulating streamflow and provides satisfactory results for sediment transport. However, the limited availability of observed suspended sediment data remains a significant challenge for achieving a more reliable and persuasive model application. The calibrated model has also been utilized to simulate nonpoint source pollution loads in the Song River catchment. With ongoing refinement and the incorporation of additional field data, the model exhibits substantial potential to improve hydrological modelling and support more effective water resource management strategies in the future.

REFERENCES

Aawar, T., and Khare, D. (2020). Assessment of climate change impacts on streamflow through hydrological model using SWAT model: a case study of Afghanistan. *Modeling Earth Systems and Environment*, *6*(3), 1427-1437.

Agrawal, N., Verma, M. K., and Tripathi, M. P. (2011). Hydrological modelling of chhokranala watershed using weather generator with SWATmodel. *Indian Journal of Soil Conservation*, *39*(2), 89-94.

Akhtar, N., Syakir Ishak, M. I., Bhawani, S. A., and Umar, K. (2021). Various natural and anthropogenic factors responsible for water quality degradation: A review. Water, 13(19), 2660.

Alam, M. I., De, S., Dutta, S., and Saha, B. (2012). Solid-acid and ionic-liquid catalyzed one-pot transformation of biorenewable substrates into a platform chemical and a promising biofuel. *RSC advances*, *2*(17), 6890-6896.

American Public Health Association (APHA), American Water Works Association (AWWA), and Water Environment Federation (WEF). (2023). Standard Methods for the Examination of Water and Wastewater (24th ed.). Washington, DC: APHA. ISBN 978-0-87553-299-8.

Angello, Z. A., Behailu, B. M., and Tränckner, J. (2020). Integral application of chemical mass balance and watershed model to estimate point and nonpoint source pollutant loads in data-scarce little akaki river, Ethiopia. *Sustainability*, *12*(17), 7084.

Arnold, J. G., and Allen, P. M. (1996). Estimating hydrologic budgets for three Illinois watersheds. Journal of hydrology, 176(1-4), 57-77.

Arnold, J. G., Srinivasan, R., Muttiah, R. S., and Williams, J. R. (1998). Large area hydrologic modeling and assessment part I: model development 1. *JAWRA Journal of the American Water Resources Association*, *34*(1), 73-89.

Berndtsson, R. (1990). Transport and sedimentation of pollutants in a river reach: A chemical mass balance approach. Water Resources Research, 26(7), 1549-1558.

Bhanot, K., Sharma, M. K., and Kaushik, R. D. (2024). Hydrochemical characterization and pCO2 dynamics in the surface waters of Himalayan River: A case study of river Alaknanda. Environmental Monitoring and Assessment, 196(11), 1-27.

Bharti, P. K., Tyagi, P. K., and Singh, V. (2014). Assessment of heavy metals in the water of Sahastradhara hill stream at Dehradun, India. International Journal of Environment, 3(3), 164-172.

Bhutiani, R., Khanna, D. R., and Rawat, S. (2014). Recent Trend in Physico-Chemical Parameters of Song River at Nepali Farm District Dehradun, Uttrakhand, India. International Journal of Research in Biosciences, Agriculture and Tech, 2, 34-44.

Bouslihim, Y., Kacimi, I., Brirhet, H., Khatati, M., Rochdi, A., Pazza, N. E. A., ... and Yaslo, Z. (2016). Hydrologic modeling using SWAT and GIS, application to subwatershed Bab-Merzouka (Sebou, Morocco). Journal of Geographic Information System, 8(1), 20-27.

Bowes, M. J., Jarvie, H. P., Halliday, S. J., Skeffington, R. A., Wade, A. J., Loewenthal, M., Gozzard, E., Newman, J. R., and Palmer-Felgate, E. J. (2015). Characterising phospho rus and nitrate inputs to a rural river using high-frequency concentration–flow relationships. Science of the Total Environment, 511, 608–620.

Brown, G. H., Sharp, M., and Tranter, M. (1996). Subglacial chemical erosion: seasonal variations in solute provenance, Haut Glacier d'Arolla, Valais, Switzerland. Annals of glaciology, 22, 25-31.

Brown, G. H., Sharp, M., and Tranter, M. (1996). Subglacial chemical erosion: seasonal variations in solute provenance, Haut Glacier d'Arolla, Valais, Switzerland. Annals of glaciology, 22, 25-31.

Brutsaert, W., and Parlange, M. B. (1998). Hydrologic cycle explains the evaporation paradox. Nature, 396(6706), 30-30.

Carpenter, S. R., Caraco, N. F., Correll, D. L., Howarth, R. W., Sharpley, A. N., and Smith, V. H. (1998). Nonpoint pollution of surface waters with phosphorus and nitrogen. Ecological applications, 8(3), 559-568.

Central Pollution Control Board. (2019). *Action Plan for Rejuvenation of River Suswa (Mothrawala to Raiwala), Dehradun.* Central Pollution Control Board, Delhi.

Chalotra, S. and. Rauthan, J. V. S. (2017). Bio-Diversity Of Phytoplankton Of Song River In Doon Valley, Uttarakhand. Review of Research Journal, vol 6.

Chen, D., Hu, M., Guo, Y., and Dahlgren, R. A. (2015). Reconstructing historical changes in phosphorus inputs to rivers from point and nonpoint sources in a rapidly developing watershed in eastern China, 1980–2010. Science of the Total Environment, 533, 196-204.

Chen, H., Teng, Y., and Wang, J. (2013). Load estimation and source apportionment of nonpoint source nitrogen and phosphorus based on integrated application of SLURP model, ECM, and RUSLE: a case study in the Jinjiang River, China. Environmental monitoring and assessment, 185, 2009-2021.

Christophersen, N., and Hooper, R. P. (1992). Multivariate analysis of stream water chemical data: The use of principal components analysis for the end-member mixing problem. *Water resources research*, *28*(1), 99-107.

Daggupati, P., Pai, N., Ale, S., Douglas-Mankin, K. R., Zeckoski, R. W., Jeong, J., ... and Youssef, M. A. (2015). A recommended calibration and validation strategy for hydrologic and water quality models. *Transactions of the ASABE*, *58*(6), 1705-1719.

Décamps, H. (2011). River networks as biodiversity hotlines. Comptes Rendus Biologies, 334(5-6), 420-434.

Folton, N., Andréassian, V., and Duperray, R. (2015). Hydrological impact of forest-fire from paired-catchment and rainfall–runoff modelling perspectives. *Hydrological Sciences Journal*, *60*(7-8), 1213-1224.

Gassman, P. W., Sadeghi, A. M., and Srinivasan, R. (2014). Applications of the SWAT model special section: overview and insights. Journal of Environmental Quality, 43(1), 1-8.

Gelete, G., Nourani, V., Gokcekus, H., and Gichamo, T. (2023). Ensemble physically based semi-distributed models for the rainfall-runoff process modeling in the data-scarce Katar catchment, Ethiopia. Journal of Hydroinformatics, 25(2), 567-592.

Ghoraba, S. M. (2015). Hydrological modeling of the Simly Dam watershed (Pakistan) using GIS and SWAT model. *Alexandria Engineering Journal*, *54*(3), 583-594.

Gibbs, R. J. (1970). Mechanisms controlling world water chemistry. Science, 170(3962), 1088–1090.

Groeschke, M., Frommen, T., Taute, T., and Schneider, M. (2017). The impact of sewage-contaminated river water on groundwater ammonium and arsenic concentrations at a riverbank filtration site in central Delhi, India. Hydrogeology journal, 25(7), 2185.

Gupta, A., Hantush, M. M., Govindaraju, R. S., and Beven, K. (2024). Evaluation of hydrological models at gauged and ungauged basins using machine learning-based limits-of-acceptability and hydrological signatures. *Journal of Hydrology*, *641*, 131774.

Hassan, M. A., Church, M., Yan, Y., and Slaymaker, O. (2010). Spatial and temporal variation of in-reach suspended sediment dynamics along the mainstem of Changjiang (Yangtze River), China. *Water Resources Research*, *46*(11).

Hooper, R. P., Christophersen, N., and Peters, N. E. (1990). Modelling streamwater chemistry as a mixture of soilwater end-members—An application to the Panola Mountain catchment, Georgia, USA. *Journal of Hydrology*, *116*(1-4), 321-343.

Ismail, W. R., Siow, A. Y., and Ali, A. (2005). Water quality and chemical mass balance of Tropical Freshwater Wetland, Beriah Swamp, Perak. Jurnal Teknologi (F), 43, 65-84.

Iwanaga, T., Partington, D., Ticehurst, J., Croke, B. F., and Jakeman, A. J. (2020). A socio-environmental model for exploring sustainable water management futures: Participatory and collaborative modelling in the Lower Campaspe catchment. Journal of Hydrology: Regional Studies, 28, 100669.

Jain, C. K. (1996). Application of chemical mass balance approach to upstream/downstream river Monitoring data. *Journal of Hydrology, 182*, 105-115.

Jain, C. K. (2000). Application of chemical mass balance approach to determine nutrient loading. Hydrological Sciences Journal, 45(4), 577-588.

Jain, C. K., Bhatia, K. K. S., and Seth, S. M. (1998). Assessment of point and non-point sources of pollution using a chemical mass balance approach. Hydrological Sciences, 43(3).

Jain, C. K., Singhal, D. C., and Sharma, M. K. (2007). Estimating nutrient loadings using chemical mass balance approach. *Environmental monitoring and assessment*, *134*, 385-396.

Jain, S. K., Tyagi, J., and Singh, V. (2010). Simulation of runoff and sediment yield for a Himalayan watershed using SWAT model. *Journal of Water Resource and Protection*, *2*(3), 267-281.

Janjić, J., and Tadić, L. (2023). Fields of application of SWAT hydrological model—a review. Earth, 4(2), 331-344.

Jindal, R., and Sharma, C. (2011). Studies on water quality of Sutlej River around Ludhiana with reference to physicochemical parameters. Environmental monitoring and assessment, 174, 417-425.

Joseph, J., Ghosh, S., Pathak, A., and Sahai, A. K. (2018). Hydrologic impacts of climate change: Comparisons between hydrological parameter uncertainty and climate model uncertainty. *Journal of Hydrology*, *566*, 1-22.

Joshi, D. M., Kumar, A., and Agrawal, N. (2009). Studies on physicochemical parameters to assess the water quality of river Ganga for drinking purpose in Haridwar district. Rasayan journal of chemistry, 2(1), 195-203.

Kaur, S., and Naseer, S. (2023). Water Quality Assessment of Sahastradhara Stream, Dehradun, Uttarakhand, India. Asian Journal of Environment and Ecology, 22(1), 29-39.

Kaur, T., and Sinha, A. K. (2019). Pesticides in agricultural run offs affecting water resources: a study of Punjab (India). Agricultural Sciences, 10(10), 1381-1395.

Kelley, D. W., and Nater, E. A. (2000). Source apportionment of lake bed sediments to watersheds in an Upper Mississippi basin using a chemical mass balance method. Catena, 41(4), 277-292.

Khadse, G. K., Patni, P. M., Kelkar, P. S., and Devotta, S. (2008). Qualitative evaluation of Kanhan river and its tributaries flowing over central Indian plateau. Environmental monitoring and assessment, 147, 83-92.

Khanna, D. R., Singh, V., Bhutiani, R., Chandra, K. S., Matta, G., and Kumar, D. (2007). A study of biotic and abiotic factors of Song River at Dehradun, Uttarakhand. Environment Conservation Journal, 8(3), 117-126.

Khatri, N., and Tyagi, S. (2015). Influences of natural and anthropogenic factors on surface and groundwater quality in rural and urban areas. Frontiers in life science, 8(1), 23-39.

Kloiber, S. M. (2006). Estimating nonpoint source pollution for the Twin Cities metropolitan area using landscape variables. Water, air, and soil pollution, 172(1), 313-335.

Koltsida, E., Mamassis, N., and Kallioras, A. (2023). Hydrological modeling using the Soil and Water Assessment Tool in urban and peri-urban environments: the case of Kifisos experimental subbasin (Athens, Greece). *Hydrology and Earth System Sciences*, *27*(4), 917-931.

Kumar, V., and Paramanik, S. (2020). Application of high-frequency spring discharge data: a case study of Mathamali spring rejuvenation in the Garhwal Himalaya. Water Supply, 20(8), 3380-3392.

Kumar, V., and Sen, S. (2023). Hydrometeorological field instrumentation in Lesser Himalaya to advance research for future water and food security. Environmental Monitoring and Assessment, 195(10), 1162.

Kumar, V., and Sen, S. (2024). Rating curve development and uncertainty analysis in mountainous watersheds for informed hydrology and resource management. Frontiers in Water, 5, 1323139.

Lai, Y. C., Yang, C. P., Hsieh, C. Y., Wu, C. Y., and Kao, C. M. (2011). Evaluation of non-point source pollution and river water quality using a multimedia two-model system. Journal of hydrology, 409(3-4), 583-595.

Leon, L. F., Soulis, E. D., Kouwen, N., and Farquhar, G. J. (2001). Nonpoint source pollution: a distributed water quality modeling approach. Water research, 35(4), 997-1007.

Makanda, K., Nzama, S., and Kanyerere, T. (2023). Assessing Feasibility of Water Resource Protection Practice at Catchment Level: A Case of the Blesbokspruit River Catchment, South Africa. Water, 15(13), 2394.

Matta, G., Naik, P., Kumar, A., Gjyli, L., Tiwari, A. K., and Machell, J. (2018). Comparative study on seasonal variation in hydro-chemical parameters of Ganga River water using comprehensive pollution index (CPI) at Rishikesh (Uttarakhand) India. Desalination and Water Treatment, 118, 87-95.

Mishra, R. R., and Saxena, S. (2024). Cities and rivers: a symbiotic relationship. In Managing Urban Rivers (pp. 3-24). Elsevier.

Mishra, R. R., and Saxena, S. (2024). Cities and rivers: a symbiotic relationship. In *Managing Urban Rivers* (pp. 3-24). Elsevier.

Mokarram, M., Saber, A., and Sheykhi, V. (2020). Effects of heavy metal contamination on river water quality due to release of industrial effluents. Journal of Cleaner Production, 277, 123380.

Moriasi, D. N., Arnold, J. G., Van Liew, M. W., Bingner, R. L., Harmel, R. D., and Veith, T. L. (2007). Model evaluation guidelines for systematic quantification of accuracy in watershed simulations. *Transactions of the ASABE*, *50*(3), 885-900.

Mosley, L. M., Zammit, B., Leyden, E., Heneker, T. M., Hipsey, M. R., Skinner, D., and Aldridge, K. T. (2012). The Impact of Extreme Low Flows on the Water Quality of the Lower Murray River and Lakes (South Australia). Water Resources Management, 26, 3923–3946.

Narsimlu, B., Gosain, A. K., Chahar, B. R., Singh, S. K., and Srivastava, P. K. (2015). SWAT model calibration and uncertainty analysis for streamflow prediction in the Kunwari River Basin, India, using sequential uncertainty fitting. *Environmental Processes*, *2*, 79-95.

Nash, J. E., and Sutcliffe, J. V. (1970). River flow forecasting through conceptual models' part I—A discussion of principles. Journal of hydrology, 10(3), 282-290.

Nguyen, H. Q., and Kappas, M. (2015). Modeling surface runoff and evapotranspiration using SWAT and beach for a tropical watershed in North Vietnam, compared to MODIS products. *International Journal of Advanced Remote Sensing and GIS*, *4*(1), 1367-1384.

Pan, B., Yuan, J., Zhang, X., Wang, Z., Chen, J., Lu, J., ... and Xu, M. (2016). A review of ecological restoration techniques in fluvial rivers. International Journal of Sediment Research, 31(2), 110-119.

Panda, P. K., Panda, R. B., and Dash, P. K. (2018). The river water pollution in India and abroad: A critical review to study the relationship among different physico-chemical parameters. American Journal of Water Resources, 6(1), 25-38.

Pandey, R. P., Kumar, P., Panday, B. K., Tyagi, J. V., Singh, R., Kumar, S., and Saini, S. (2021). Development of rejuvenation plan for Rispana river system, Uttarakhand, India. Water and Energy International, 64(2), 6-18.

Pankaj, A., and Kumar, P. (2009). GIS-based morphometric analysis of five major sub-watersheds of Song River, Dehradun District, Uttarakhand with special reference to landslide incidences. Journal of the Indian Society of Remote Sensing, 37, 157-166.

Parker, H., and Oates, N. (2016). How do healthy rivers benefit society. A Review of the Evidence. London: ODI and WWF.

Pérez-Sánchez, J., Senent-Aparicio, J., Segura-Méndez, F., Pulido-Velazquez, D., and Srinivasan, R. (2019). Evaluating hydrological models for deriving water resources in peninsular Spain. Sustainability, 11(10), 2872.

Phuong, T. T., Thong, C. V. T., Ngoc, N. B., and Van Chuong, H. (2014). Modeling soil erosion within small mountainous watershed in central Vietnam using GIS and SWAT. *Resour. Environ*, *4*(3), 139-147.

Quamar, S., Kumar, P., and Singh, H. P. (2025). Streamflow and sediment simulation in the Song River basin using the SWAT model. Frontiers in Water, 7, 1500086.

Rafiei Emam, A., Kappas, M., Linh, N. H. K., and Renchin, T. (2017). Hydrological modeling and runoff mitigation in an ungauged basin of central Vietnam using SWAT model. *Hydrology*, *4*(1), 16.

Rakesh, P., Samiksha, K., Harmanpreet, K., Mansi, R., Vijay, K., and Amit, G. (2022). Qualitative and quantitative enumeration of Coliform bacteria in song river water in rural area of Dehradun. environments, 1, 2.

Razali, A., Syed Ismail, S. N., Awang, S., Praveena, S. M., and Zainal Abidin, E. (2018). Land use change in highland area and its impact on river water quality: a review of case studies in Malaysia. Ecological processes, 7, 1-17.

Reinelt, L. E., and Grimvall, A. (1992). Estimation of nonpoint source loadings with data obtained from limited sampling programs. Environmental monitoring and assessment, 21, 173-192.

Sahu, M., Lahari, S., Gosain, A. K., and Ohri, A. (2016). Hydrological modeling of Mahi basin using SWAT. *Journal of Water Resource and Hydraulic Engineering*, *5*, 68-79.

Samimi, M. (2020). *Adaptive Agricultural Water Resources Management in a Desert River Basin: Insights from Hydrologic Modeling* (Doctoral dissertation, Oklahoma State University).

Sanap, R. R., Mohite, A. K., Pingle, S. D., and Gunale, V. R. (2006). Evaluation of water qualities of Godawari River with reference to physico-chemical parameters, Dist. Nasik (MS), India. Pollution Research, 25(4), 775.

Sane, M. L., Sambou, S., Leye, I., Ndione, D. M., Diatta, S., Ndiaye, I., ... and Kane, S. (2020). Calibration and Validation of the SWAT Model on the Watershed of Bafing River, Main Upstream Tributary of Senegal River: Checking for the Influence of the Period of Study. Open Journal of Modern Hydrology, 10(4), 81-104.

Santy, S., Mujumdar, P., and Bala, G. (2020). Potential impacts of climate and land use change on the water quality of Ganga River around the industrialized Kanpur region. Scientific reports, 10(1), 9107.

Schuol, J., Abbaspour, K. C., Yang, H., Srinivasan, R., and Zehnder, A. J. (2008). Modelling blue and green water availability in Africa. *Water resources research*, *44*(7).

Seneviratne, S. I., Corti, T., Davin, E. L., Hirschi, M., Jaeger, E. B., Lehner, I., ... and Teuling, A. J. (2010). Investigating soil moisture–climate interactions in a changing climate: A review. Earth-Science Reviews, 99(3-4), 125-161.

Sharma, M.K., Kumar, P., Bhanot, K., and Prajapati, P. (2021). Assessment of non-point source of pollution using chemical mass balance approach: a case study of River Alaknanda, a tributary of River Ganga, India. Environmental monitoring and assessment, 193, 424 (2021). https://doi.org/10.1007/s10661-021-09203-x

Sharma, N., Rayal, R., and Bahuguna, P. (2022). The Impact of Physicochemical Parameters on The Density And Diversity of Water Mite Communities of The Downstream Zone of Song River in Dehradun, Uttarakhand. J. Mountain. Res, 17(2), 269-278.

Shen, Z., Hong, Q., Yu, H., and Liu, R. (2008). Parameter uncertainty analysis of the non-point source pollution in the Daning River watershed of the Three Gorges Reservoir Region, China. Science of the total environment, 405(1-3), 195-205.

Shen, Z., Zhong, Y., Huang, Q., and Chen, L. (2015). Identifying non-point source priority management areas in watersheds with multiple functional zones. Water research, 68, 563-571.

Singh, O., Arya, P., and Chaudhary, B. S. (2013). On rising temperature trends at Dehradun in Doon valley of Uttarakhand, India. Journal of Earth System Science, 122, 613-622.

Singh, V. K., Singh, K. P., and Mohan, D. (2005). Status of heavy metals in water and bed sediments of river Gomti–A tributary of the Ganga river, India. Environmental monitoring and assessment, 105, 43-67.

Srinivas, R., Singh, A. P., Dhadse, K., and Garg, C. (2020). An evidence based integrated watershed modelling system to assess the impact of non-point source pollution in the riverine ecosystem. Journal of cleaner production, 246, 118963.

Suryavanshi, S., Pandey, A., and Chaube, U. C. (2017). Hydrological simulation of the Betwa River basin (India) using the SWAT model. *Hydrological Sciences Journal*, *62*(6), 960-978.

Suthar, S., Sharma, J., Chabukdhara, M., and Nema, A. K. (2010). Water quality assessment of river Hindon at Ghaziabad, India: impact of industrial and urban wastewater. Environmental monitoring and assessment, 165, 103-112.

Swain, S., Mishra, S. K., Pandey, A., Pandey, A. C., Jain, A., Chauhan, S. K., and Badoni, A. K. (2022). Hydrological modelling through SWAT over a Himalayan catchment using high-resolution geospatial inputs. Environmental Challenges, 8, 100579.

Tikuye, B. G., Gill, L., Rusnak, M., and Manjunatha, B. R. (2023). Modelling the impacts of changing land use and climate on sediment and nutrient retention in Lake Tana Basin, Upper Blue Nile River Basin, Ethiopia. Ecological Modelling, 482, 110383.

Usha, K., and Singh, B. (2024). Reifying "Yamuna": Unpacking the Pluriversal Possibilities for Rejuvenation of the River at Poiaghat, Swarg Dhaam, Agra. PARITANTRA, 40.

Vandenberghe, V., Van Griensven, A., Bauwens, W., and Vanrolleghem, P. A. (2006). Effect of different river water quality model concepts used for river basin management decisions. *Water science and technology*, *53*(10), 277-284.

Wang, G., Li, J., Sun, W., Xue, B., Yinglan, A., and Liu, T. (2019). Non-point source pollution risks in a drinking water protection zone based on remote sensing data embedded within a nutrient budget model. Water research, 157, 238-246.

Withers, P. J. A., and Jarvie, H. P. (2008). Delivery and cycling of phosphorus in rivers: a review. Science of the total environment, 400(1-3), 379-395.

Wu, Y., and Chen, J. (2013). Investigating the effects of point source and nonpoint source pollution on the water quality of the East River (Dongjiang) in South China. Ecological indicators, 32, 294-304.

Zhai, X., Zhang, Y., Wang, X., Xia, J., and Liang, T. (2014). Non-point source pollution modelling using Soil and Water Assessment Tool and its parameter sensitivity analysis in Xin'anjiang catchment, China. Hydrological Processes, 28(4), 1627-1640.

ACKNOWLEDGEMENTS

The authors sincerely acknowledge the Department of Water Resources, River Development and Ganga Rejuvenation, Ministry of Jal Shakti for providing the financial support for conducting this research work.

The authors sincerely recognize the Central Water Commission for providing the discharge and cross-sections data required for the analysis.

The authors wish to thank the Director, National Institute of Hydrology Roorkee, Uttarakhand as well as the Head, Environmental Hydrology Division for for providing all administrative and financial support for the successful completion of the project and providing NABL accredited water quality lab to conduct the research work.